

# **Influence of Kv11.1 (hERG1) K<sup>+</sup> channel expression on DNA damage induced by the genotoxic agent methyl methanesulfonate**

Sara Fernández-Villabrille<sup>1,2</sup>, Enol Álvarez-González<sup>1</sup>, Francisco Barros<sup>2</sup>, Pilar de la Peña<sup>2</sup>  
and L. María Sierra<sup>1</sup>

<sup>1</sup> Departamento de Biología Funcional (Area de Genética), Instituto Universitario de Oncología del Principado de Asturias (IUOPA), Instituto de Investigación Sanitaria del Principado de Asturias (ISPA); Universidad de Oviedo, 33006 Oviedo, Asturias, Spain.

<sup>2</sup> Departamento de Bioquímica y Biología Molecular, Universidad de Oviedo, Edificio Santiago Gascón, Campus de El Cristo, 33006 Oviedo (Asturias), Spain

Running title: **hERG and MMS-induced DNA damage**

## **Address correspondence to:**

<sup>1</sup>Luisa Maria Sierra.

Departamento de Biología Funcional (Area de Genética), Universidad de Oviedo, 33006 Oviedo, Asturias, Spain.

Email: [lsierra@uniovi.es](mailto:lsierra@uniovi.es) (+34 985102723)

Orcid: 0000-0002-9046-1171

## **Acknowledgements**

We thank the expert technical contribution of Teresa González. LMS pertains to the Mass Spectrometry & Biomedical Analysis group of the University of Oviedo and was supported by Grant MINECO CTQ2016-80069-C2-1-R from the Ministerio de Economía y Competitividad of Spain. FB and PdIP work at the Hormone Receptors and Ion Channels group of the University of Oviedo and were supported in part by Grant BFU2015-66429-P (MINECO/FEDER UE) from the Spanish Ministerio de Economía y Competitividad, co-financed with European Fund for Economic and Regional Development (FEDER) funds. EAG held a Ph.D. Bridge B fellowship from the University of Oviedo. Authors would like to acknowledge the technical support provided by the Scientific-Technical Services (SCTs) of the University of Oviedo.

## **ABSTRACT**

Besides their crucial role in cell electrogenesis and maintenance of basal membrane potential, the voltage-dependent K<sup>+</sup> channel Kv11.1/hERG1 shows an essential impact in cell proliferation and other processes linked to the maintenance of tumour phenotype. To check the possible influence of channel expression on DNA damage responses, HEK293 cells, treated with the genotoxic agent methyl methanesulfonate (MMS), were compared with those of a HEK-derived cell line (H36), permanently transfected with the Kv11.1-encoding gene, and with a third cell line (T2) obtained under identical conditions as H36, by permanent transfection of another unrelated plasma membrane protein encoding gene. In addition, to gain some insights about the canonical/conduction-dependent channel mechanisms that might be involved, the specific erg channel inhibitor E4031 was used as a tool. Our results indicate that the expression of Kv11.1 does not influence MMS-induced changes in cell cycle progression, because no differences were found between H36 and T2 cells. However, the canonical ion conduction function of the channel appeared to be associated with decreased cell viability at low/medium MMS concentrations. Moreover, direct DNA damage measurements, using the comet assay, demonstrated for the first time that Kv11.1 conduction activity was able to modify MMS-induced DNA damage, decreasing it particularly at high MMS concentration, in a way related to *PARP1* gene expression. Finally, our data suggest that the canonical Kv11.1 effects may be relevant for tumour cell responses to anti-tumour therapies.

## **Keywords**

hERG channel, Kv11.1, methyl methanesulfonate, DNA damage, apoptosis, cell cycle progression, cell viability, PARP1 gene expression, clonogenic efficiency

## INTRODUCTION

Ion channels are transmembrane proteins crucially involved in the maintenance of plasma membrane potentials, electrical excitability, cellular electrogenesis and ionic homeostasis [37]. However, they have been recently involved also in other physiological processes such as regulation of intracellular pH and cell volume, proliferation, migration, differentiation, and control of cell cycle and apoptosis [36,40]. Furthermore, their alteration and/or deregulation in some cell types has been recognized as a cause of tumour progression [65]. Indeed, several ionic channels are involved in the manifestation of pathophysiological characteristics known as hallmarks of cancer [7,73]. Strikingly, in addition to the effects mediated by ion channels canonical functions, allowing ions to cross the membrane and/or modulating membrane potential, the influence of ion channels on cell functions that, for example favour tumour progression, might be achieved both via canonical ion-conducting characteristics involving ion permeation, and/or through non-canonical mechanisms independent from ion conduction [21,46,64,73,89,91]. These mechanisms can include direct physical interactions with other proteins or molecules entailed in intracellular signalling [11]. Also, ion channels are considered attractive therapeutic targets in cancer [25,69], as well as markers for malignant transformation, provided that their expression is altered in tumours [52,55].

Among ion channels, potassium channels, and more specifically voltage-dependent ones (Kvs), constitute one of the groups more frequently involved in those cell functions that favour tumour progression (reviewed in [17,36,52,69,73]). The EAG or KCNH family [5,33,77], and especially two of its members, Kv10.1 (eag1, encoded by the human gene *KCNH1*) and Kv11.1 (erg1, encoded by the gene *KCNH2*, here also called hERG1 for simplicity), demonstrated their aberrant expression in a variety of tumour cells, where they increased cell proliferation and tumour malignancy [3,17,54,69,73].

Specifically, Kv11.1 is a channel with a fundamental physiological role chiefly in cardiac cells, but also in other cell types such as smooth muscle, neuronal, and neuroendocrine cells, in which its impact in crucial cell functions (e.g. contraction, electrical excitability and hormone secretion) has been quite exhaustively studied [2,5,6,86]. However, the expression of the channel has also been associated to some characteristics of tumour progression, such as tumour cell proliferation [53,71], angiogenesis, cell migration, and differentiation (reviewed in [17,73]). Furthermore, hERG1 channel over-expression has been detected in several tumour cell lines (e.g. leukemic, epithelial and connective tissue cells) and in several types of primary tumours but not in their corresponding healthy tissues [54,71], and it has been associated to poor prognosis in some tumours [17].

Some of these functions in tumour progression might be exerted through canonical mechanisms, derived from the  $K^+$  permeation property of the channel because, as for other  $K^+$  channels, Kv11.1 activity is crucial for the maintenance of membrane polarization. Thus, variations in basal membrane potential may impact cell differentiation, tumour progression and intracellular homeostasis of  $Ca^{2+}$  [62,90,91], an ion that seems to play a role in the action of some DNA-damaging agents [24,32]. Nevertheless, in the case of Kv11.1, some non-canonical actions independent of ion flux activity, probably through direct interactions with other signalling protein elements, have been recognized on cell proliferation, migration, apoptosis or cell cycle progression events [1,30,56,57,88].

A generalized and straightforward approach to determine the influence of Kv11.1 canonical function is to use specific channel inhibitors, such as E4031, a class III antiarrhythmic agent able to specifically block the  $K^+$  conducting activity of the erg channels at nanomolar concentrations [49,83,92,94]. Using this inhibitor, some works reported that pharmacological blockade of Kv11.1 currents in several types of tumour cells reduced cell proliferation [1,53,71,72], decreased cell migration and lowered intracellular  $Ca^{2+}$  levels [56], and inhibited the growth of xenograft implants of human tumour cells from stomach cancer [3]. The use of E4031 also demonstrated that tumour cell proliferation and/or viability were not affected by hERG1 current blockade in some tumour cell lines, although they were reduced by hERG1 knockdown using siRNAs [30,57]. In other cases, however, the use of E4031 showed that mixed canonical and non-canonical hERG1 effects were responsible for decreased VEGF secretion in cell lines from colorectal cancers [18].

Despite all the information available about the influence of Kv11.1 on tumour progression, there is little direct information on whether this channel influences DNA damage responses, because the analyses were mostly centred in cellular responses such as cytotoxicity, cell proliferation, migration and/or apoptosis [1,13,30,56,57,71,72,88,93], but not in the induced DNA damage itself. Because of this, in this study we interrogated the possible influence of Kv11.1 on DNA damage responses, focusing the analysis on the DNA damage induced by a genotoxic agent, and checking whether canonical or non-canonical hERG1 mechanisms were involved using E4031 as a tool. The monofunctional alkylating agent methyl methanesulfonate (MMS) chosen for this work is a genotoxic agent used as a model chemical since many years, able to induce apoptosis and cell cycle alterations, and with a well-known mechanism of action on the DNA [9,29,34,43,63,84]. MMS methylates mainly nitrogen atoms of nitrogen DNA bases, such as N7-G and N3-A, that may release apurinic site intermediates *in vitro* and *in vivo* [9]. Consequently, MMS induces both base-pair changes and deletions in different cell types and organisms [50,51,63].

The MMS-induced DNA damage was determined using the comet assay (*single-cell gel electrophoresis* or SCGE) that detects single and double DNA strand breaks [15]. Such strand breaks can be induced: (i) either directly; (ii) by labilization of alkali-labile abasic (apurinic/apirimidinic) site intermediates of different DNA damage types; (iii) by the activity of DNA damage excision repair systems; and/or (iv) by replication blockages [47]. This assay quantifies DNA damage in individual cells in a simple, rapid, and easy way [80], and has been systematically used to determine DNA damage and DNA repair [15,61,79] in different types of cells and organisms [20,26-28], biomonitoring human populations [4], or in ecogenotoxicology studies [10].

Finally, to know the impact on DNA damage caused by the presence of Kv11.1, we compared HEK293 cells, lacking the channel, with those of the derived cell line HEK-H36 (named H36 through the text), obtained by permanent transfection of the HEK293 cells with the Kv11.1-encoding gene [59]. Additionally, as a permanent transfection control, we used the cell line HEK-TRHR2 (named T2), in which an unrelated plasma membrane protein (the thyrotropin-releasing hormone receptor) is over-expressed, after permanent transfection with its coding gene under identical conditions to those used to obtain H36 cells.

Our results demonstrate for the first time that the expression of Kv11.1 can modify the level of induced DNA damage, particularly at high MMS concentration, and also the cell viability and clonogenic efficiency after treatment with this genotoxic agent. They also indicate that the presence of hERG1 does not influence MMS-induced cell cycle progression. Moreover, they show that the Kv11.1 effects on induced DNA damage and in cell viability are linked to its canonical function as an ion channel, and that those on DNA damage might be related to Kv11.1-dependent different DNA repair activities, like expression of the *PARP1* gene. Importantly, our data alert about the convenience of using E4031 under appropriate depolarizing conditions to ensure channel opening and complete inhibition of its activity. Finally, they also suggest that the canonical Kv11.1 effects may be relevant for tumour cell responses to anti-tumour therapies.

## **MATERIAL AND METHODS**

### **Generation of permanently transfected HEK293 cell clones and culturing conditions.**

Generation of H36 cells permanently expressing Kv11.1 channels has been described elsewhere [59]. Briefly, monolayer cultures ( $\approx 50\%$  confluent) of human embryonic kidney cells (HEK293; ATCC CRL-1573) were transfected with Kv11.1 channel cDNA subcloned into *HindIII/BamHI* sites of the pcDNA3 vector (Invitrogen), using Lipofectamine (Gibco).

Three days after transfection, the cells were trypsinized and diluted in a medium containing 1 mg/ml geneticin. Subsequently, they were cultured until cell colonies were visible. Individual colonies were picked with cloning cylinders and electrophysiologically tested for Kv11.1 currents. Cells of clone H36, showing robust currents under voltage-clamp, were selected for the experiments. T2 cells were obtained in the same way using a pcDNA3.1/Hygro(+) plasmid (Invitrogen), containing the cDNA for the thyrotropin releasing hormone receptor (TRH-R, [19]) inserted between the *HindIII/XbaI* sites of the vector. In this case, Hygromycin B (150 µg/ml) was used to select, as above, individual clones expressing the receptors. We chose for further work the clone named T2, exhibiting prominent and reproducible calcium responses when perfused with TRH after loading the cells with the fluorescent Ca<sup>2+</sup> indicator Fura-2 [59].

All cell lines were grown at 37°C in a humidified atmosphere of 95% air and 5% CO<sub>2</sub> using a 1:1 mixture of Dulbecco's modified Eagle's medium and Ham's F-12 nutrient mixture (Sigma), supplemented with 100 U/ml penicillin, 1.1 mg/ml streptomycin and 10% fetal bovine serum. The doubling time was approximately 24 h for the HEK293 and 36 h for the H36 and T2 cells under these conditions. Antibiotics used for selection were not employed during subsequent studies. Thus, only cells from passages 3-10 after thawing were utilized, to ensure that channel expression was maintained, as demonstrated by systematic testing of Kv11.1-type ionic currents presence in the H36 cells used for the experiments.

### **Electrophysiological recordings and intracellular calcium measurements.**

Ion current recordings and estimations of cell membrane potential were performed at room temperature under voltage-clamp and current-clamp conditions, respectively. The perforated-patch variant of the patch-clamp technique was used to minimize alterations of intracellular content. Perforation of the patches was achieved using nystatin as detailed elsewhere [12,59]. Electrodes were filled with a solution containing (in mM): 65 KCl, 30 K<sub>2</sub>SO<sub>4</sub>, 10 NaCl, 1 MgCl<sub>2</sub>, 50 sucrose and 10 Hepes (pH7.4 with KOH). The standard extracellular saline used for recordings contained (in mM): 137 NaCl, 4 KCl, 1.8 CaCl<sub>2</sub>, 1 MgCl<sub>2</sub>, 10 glucose, 10 HEPES (pH 7.4 with NaOH). When indicated, a depolarizing extracellular saline was employed, in which NaCl was substituted by 136 mM KCl. The voltage dependence of Kv11.1 current activation in H36 cells was assessed using standard tail current analysis. Tail current magnitudes normalized to maximum were fitted with a Boltzmann function:  $h(V) = I_{\max} / [1 + \exp((V - V_{1/2})/k)]$ , where V is the test potential, V<sub>1/2</sub> is the half-activation voltage, and k is the slope factor. Typical ionic currents, with the kinetic

and biophysical characteristics of hERG, were observed in all recorded H36 cells used, but were never observed in HEK293 and T2 cells. Procedures for cell loading with the Ca<sup>2+</sup>-sensitive dye Fura-2 and for measurements of variations in intracellular Ca<sup>2+</sup> concentrations ([Ca<sup>2+</sup>]<sub>i</sub>), to establish maintenance of TRH-R expression in T2 cells, have been detailed elsewhere [12,59].

### **Chemical agents**

Methyl methanesulfonate, MMS (CAS N° 66-27-3), obtained from Sigma-Aldrich, Spain, was dissolved in sterile purified distilled water to prepare 10 mM stock solutions immediately before the experiments. 1 mM stock solutions of the Kv11.1 current inhibitor E4031 (CAS N° 113558-89-7; Sigma-Aldrich, Spain) in sterile distilled water were stored at -20°C. The working concentration was subsequently prepared in cell culture medium or extracellular saline when indicated. 5 µM E4031 was used for all treatments in serum-containing cultured media. The compound was continuously perfused to the recording chamber at a more reduced concentration of 1 µM, dissolved in the extracellular saline used for the patch-clamp electrophysiological experiments.

### **MTS viability and clonogenic assays**

Variations in cell viability levels induced by MMS treatment were determined in 96 well plates using the MTS CellTiter 96<sup>®</sup> Aqueous One Solution Cell Proliferation Assay (Promega). Cells were seeded at 10<sup>4</sup> cells/well density in 0.1 ml of medium and cultured during 48 h. They were subsequently treated with various MMS concentrations, between 0.01 and 0.6 mM, as indicated in the corresponding results. Six wells were used for each concentration assayed. After 3 h of treatment, cells were washed twice with phosphate buffered saline (PBS) and covered with 0.1 ml of fresh medium. After an additional 24 h incubation, 20 µl of MTS per well were added and the absorbance at 490 nm was measured one hour later with a VariosKan Flash spectrophotometer (Thermo Scientific). Viability values were obtained using SKantIt<sup>®</sup> software (Thermo Scientific). At least two independent experiments were performed for each cell line and concentration. To study the impact of E4031 on MMS-induced changes on viability, 5 µM of the inhibitor was added to each well as indicated, together with the corresponding MMS concentrations.

For clonogenic survival analysis, 10<sup>5</sup> cells/well were seeded in a 6-well plate for 24 hours and then treated for 3 h at 37°C in culture medium with the indicated concentrations of MMS. Immediately after treatment 1,000 or 3,000 cells per well were re-plated in new 6-well plates to assess colony forming efficiency. The plates were left in the incubator for

6-10 days until clones of at least 50 cells appeared. The cells were washed with PBS, fixed with methanol:acetic acid (3:1) for 5 min, and stained with 0.5% crystal violet in methanol for 15 min. The dye mixture was removed, the plates rinsed with tap water, and the colony numbers were counted after drying.

### **Estimation of DNA damage levels using the comet assay.**

Six-well plates were used to seed the cells at  $0.5 \times 10^6$  cells/well. After 72 h, cells were treated with the indicated concentrations of MMS. Negative controls with only culture medium were always run in parallel. After a 3 h treatment, cells were washed twice with PBS, trypsinized and suspended in PBS at  $3.3 \times 10^6$  cells/ml. The alkaline Comet assay was performed as previously described [23]. Briefly,  $10^5$  cells in 0.5% low melting point (LMP) agarose (Invitrogen) were spread on slides precoated with 0.5% of normal melting point (NMP) agarose (Invitrogen). These gels were subjected to 1 h lysis (89% of NaCl 2.5 M, Na<sub>2</sub>EDTA 100 mM, Tris 10 mM, NaOH 0.25 M, pH=10, 10% of DMSO and 1% Triton X-100), 20 min denaturing at pH>13 (Na<sub>2</sub>EDTA 1 mM and NaOH 300 mM), and 20 min electrophoresis at 0.81 V/cm and 300 mA, at 4°C in the dark. After 3 x 5 min neutralization with 0.4 M Tris-HCl, pH 7.5, and 5 min fixation with absolute ethanol, each slide was coded for blind analysis and gels were stained with 40 µl of ethidium bromide (0.5 µg/ml) and 1 µl of fluorescence protector Vectashield® (VECTOR laboratories, Inc. Burlingame). Nucleoids were visualized at 400x magnification with an Olympus BX61 fluorescence microscope, equipped with fluorescence filters and an Olympus DP70 CCD-coupled camera at the Scientific-Technical Services (SCTs) of our University. Nucleoids from at least 50 cells per gel were scored and photographs were analysed with the Komet 5 software program (Kinetic, UK). Two gels were analysed *per* MMS concentration, and at least three independent experiments were carried out for each concentration, condition and cell line. The percentage of DNA on nucleoid tails (% Tail DNA) was used as the Comet assay parameter.

The effect of E4031 on DNA damage was determined, as described for the viability, adding this chemical in co-treatments with the corresponding MMS concentrations. When indicated, it was also used for 5 min pre-incubations in depolarizing high KCl extracellular saline, before changing the medium for the co-treatments with MMS.

To check DNA repair activity, the comet assay was also used to assess the disappearance of 0.2 mM MMS-induced DNA damage in HEK293 and H36 cells. In this case, after the standard 3 h treatment with MMS, cells were washed two times with PBS,

allowed to recover in new fresh culture medium for different time periods (30 min, 1 hour and 2 hours), and then cells were harvested to perform the comet assay as described above. Two independent experiments were carried out for each cell line.

### **Cell apoptosis and cell cycle assays.**

Cells were seeded in six-well plates at  $7 \times 10^5$  cells/well and cultured 24 h before performing 3 h treatments with four different MMS concentrations (0.05, 0.1, 0.2 and 0.35 mM), and only with the solvent (negative control). Following the treatments, cells were washed twice with PBS and incubated 24 h with fresh medium without the agent. Next, they were trypsinized and divided in  $10^5$  and  $5 \times 10^5$  aliquots for apoptosis and cell cycle analysis, respectively. The Annexin V-Fluorescein isothiocyanate (FITC) apoptosis detection method (Immunostep, Spain) was used for cell apoptosis analysis. Briefly,  $10^5$  cells were resuspended in 0.2 ml of a solution containing 2  $\mu$ l of annexin V-FITC BioVision<sup>®</sup> reagent, 14  $\mu$ l of 0.1 mg/ml propidium iodide (PI) and 184  $\mu$ l of Annexin-binding buffer (140 mM NaCl, 2.5 mM CaCl<sub>2</sub>, 10 mM Hepes/NaOH pH 7.4). Cells were incubated for 15 min at room temperature in the dark, and apoptosis levels were determined with a Cytoflex S cytometer (Beckman Coulter) and CytExpert<sup>®</sup> analysis software (Beckman Coulter), at the SCTs from the University of Oviedo. For cell cycle analysis, 0.5 ml of PBS was added to  $5 \times 10^5$  treated cells and then the cells were fixed by adding 2 ml of cold 70% ethanol and frozen at -20°C for at least 24 h. Afterwards, the cells were centrifuged to eliminate ethanol and resuspended in a solution containing 50  $\mu$ l of PBS, 50  $\mu$ l of 10  $\mu$ g/ml RNase and 75  $\mu$ l of 140  $\mu$ g/ml PI. After 30 min in the dark at room temperature, cells were analysed in the Cytoflex S cytometer, using “ModFit LT” (Verity Software House).

### **Estimation of *PARP1* expression.**

To estimate the level of *PARP1* expression in HEK293 and H36 cells, RNA extraction and reverse transcription was achieved by extracting global RNA from  $2-4 \times 10^6$  cells, treated in T-25 flasks for each cell type and analysed condition (untreated and treated with 0.2 mM MMS), using the RNA purification kit E.Z.N.A.<sup>®</sup> Total RNA Kit I (Omega bio-tek), combined with a DNA digestion with E.Z.N.A. RNase-Free DNase I Set (Omega bio-tek), according to the manufacturer’s instructions. Each extraction was eluted in 50  $\mu$ l of nuclease-free H<sub>2</sub>O provided with the kit. RNA concentration and integrity were measured with Agilent RNA 6000 Nano Kit (Agilent Technologies, Inc.) in an Agilent 2100 Bioanalyzer (Agilent Technologies, Inc.), at the SCTs of the University of Oviedo,

obtaining RNA Integrity Numbers (RIN) between 8.60 and 9.50 for all the samples. Reverse transcription was performed using RevertAid H Minus First Strand cDNA Synthesis Kit (ThermoFisher Scientific) following the manufacturer's indications, with 3.11 µg of RNA from each cell type and analysed conditions, and using oligo-dT as primer.

Differential gene expression of *PARP1* gene in HEK293 and H36 cells, untreated and treated ones, was analyzed by qPCR with the TaqMan® gene expression assay Hs00242302\_m1 (Applied Biosystems), using *GAPDH* gene (Hs99999905\_m1) as reference gene with constitutive expression. The qPCR was carried out in a 7900HT Fast Real-Time PCR System (Applied Biosystems), at the SCTs of our University, using 10 µl TaqMan Universal Mastermix II with UNG (Applied Biosystems) in 20 µl of final volume, with 1 µl of Taqman probe and 2 µl of 1:4 diluted cDNA per reaction, and the following program: 50°C for 2 min, 95°C for 10 min, and 40 cycles at 95°C for 15 s and 60°C for 1 min. Using the Expression Suite Software v1.0.3 (Applied Biosystems), data were first corrected considering the reference gene, and then analysed with the relative quantification (RQ) method, which represents the fold change against the cells or treatment condition used as calibrator in each analysis, in this case control HEK293 cells. Three technical replicates were done per sample and three independent experiments were carried out, calculating the mean fold change and its standard error.

### **Statistical analysis.**

Data in the text and the figures represent arithmetic means and their SEM for the number of indicated cells. Pairwise comparisons of results were carried out with parametric unpaired (2-tailed) Student *t* tests when indicated. When significant differences in standard deviation were present an alternate Welch's test or non-parametric Wilcoxon test were also used. For the Comet assay analysis, the effects of MMS at each concentration were compared to the negative control, in individual experiments, using the non-parametric U Mann-Whitney test, because the % Tail DNA parameter does not follow a normal distribution. For multiple pairwise comparisons within one experiment one-way ANOVA and Student-Newman-Keuls (SNK) and/or HSD Tukey post-hoc tests were used as indicated. Linear regression analyses of dose-response data were also performed to check if the MMS effects depended on the concentration. Half-maximal inhibitory concentration (IC<sub>50</sub>) values were estimated with Probit analysis to obtain linear dose-response relationships. Alternatively, Hill model fits to the experimental dose-response data were performed with the eeFit add-in for Microsoft Excel [87], using nonlinear least-squares regressions with a sigmoidal function [ $y = Max - (Max - Min) (x^h / (x^h + K^h))$ ], where *K* and

$h$  are the  $IC_{50}$  value and the Hill coefficient, respectively. All the statistical tests were performed with GraphPad InStat (version 3.05) and IBM SPSS Statistics (version 21.0.0.0). In all cases,  $p$ -values  $<0.05$  were considered as indicative of statistical significance.

## RESULTS

### **Morphological and electrophysiological characterization of HEK293, H36 and T2 cells.**

Our main goal was to check the contribution of Kv11.1 to cell response(s) associated to possible DNA damage induced by sub-toxic concentrations of the genotoxic agent MMS. We analysed the cell response performing determinations of cell viability, combined with analyses of apoptosis and cell cycle progression by flow cytometry, and especially with Comet assay analysis to detect and quantify DNA damage, as an indication of induced genomic instability. To this end, we compared HEK293 cells with those of the H36 cell clone derived from them, permanently transfected with the Kv11.1-codifying gene. The T2 clone, also derived from HEK293 and permanently expressing a hormonal membrane receptor (the TRH receptor), was used as a transfection control.

As an initial step, an electrophysiological analysis was carried out to demonstrate the functional expression of Kv11.1 in H36 cells, and the complete absence of this channel currents in both HEK293 and T2 cells. As shown in Figure 1A, no obvious morphological differences were observed between the three cell types in culture. On the other hand, Figure 1B demonstrates that, after application of depolarization pulses under voltage-clamp conditions, from a basal potential of -80 mV to different voltages between -60 and +40 mV, followed by a repolarization step to -50 mV, prominent ionic currents, with the kinetic and biophysical characteristics of Kv11.1, were observed in H36 cells. Noticeably, such currents were completely absent in HEK293 and T2 cells, in which only small outwardly rectifying currents were observed during the depolarization steps, due to the activity of the endogenous voltage dependent ion channels present in these cells. Indeed, at the time scale used, in HEK293 and T2 cells a complete absence of ionic currents was apparent during the -50 mV steps. In contrast, strong outward currents were present during the same steps in H36 cells. In fact, the magnitude of these currents at the peak (black circle in Figure 1B) is clearly higher than that at the end of the previous depolarizations to positive voltages (white circle in Figure 1B), even though the electromotive force for  $K^+$  is smaller at -50 mV, given the transmembrane cation concentrations present during the recordings. This phenomenon is exclusively related to the known anomalous rectification properties of the Kv11.1 channels at positive voltages, due to very fast inactivation during depolarizing

voltage steps, and release from inactivation faster than deactivation during repolarizing voltage pulses [82,86], as demonstrated by the N-shaped current-voltage relationships exhibited by the currents when measured at the end of the depolarizing pulses (left lower panel in Figure 1B). Finally, the conductance/voltage relationships obtained by tail current analysis (right lower panel in Figure 1B) yielded a  $V_{0.5}$  value of  $-12.3 \pm 1.3$  mV ( $n=11$ ), analogous to that obtained in other studies in which Kv11.1 channel activity were recorded in similar conditions [53,75]. Altogether, these data demonstrated that the Kv11.1 channels were expressed in H36, but not in the HEK293 and the T2 cell lines.

As an additional characterization step, we also determined the possible impact of MMS, on the Kv11.1 channels expressed in H36 cells. As shown in Figure 1C, the magnitude of the Kv11.1 currents and their kinetic properties, remained unaltered both following the direct addition of 0.35 mM MMS to the recording chamber, or after a standard 3 hour treatment of the cells with 0.35 mM of the chemical, the highest agent concentration used in most of the performed functional studies (see below).

Next, the basal membrane potential ( $E_m$ ) values of the different cell lines were determined under current-clamp conditions (see Methods). The observed values were  $-61.4 \pm 3.2$  mV ( $n=8$ ) for H36,  $-35.0 \pm 1.9$  mV ( $n=5$ ) for HEK293, and  $-37.5 \pm 3.0$  mV ( $n=6$ ) for T2 (Figure 2). These results indicated that, due to the presence of the over-expressed Kv11.1 channels in H36 cells, the resting membrane potential of these cells was significantly more negative than those of HEK293 and T2 cells, that otherwise exhibited very similar values. Since in all the cases the same ionic conditions were used, corresponding to a Nernst equilibrium potential for  $K^+$  of around -90 mV, our data demonstrated that the cells expressing Kv11.1 exhibited a basal membrane potential closer to this value than the other two cell lines. An additional demonstration that these differences were due to the presence of hERG1 was provided by the fact that, as shown in Figure 2, the H36  $E_m$  value became analogous to those of the HEK293 and T2 cells, when the H36 cells were incubated with the specific erg channels inhibitor E4031, under conditions in which an almost complete blockade of the hERG1 currents is achieved [e.g. after a 5 min treatment with the inhibitor in high-KCl saline, followed by a 3 h exposition of the cells to E4031 in standard culture medium (marked *3h + KCl pulse* in the graph. See also below)].

As a final checkup, we also verified that the basal membrane potential of H36 cells was not modified following a 3 h treatment with 0.35 mM MMS. Thus, consistent with the lack of effect on the hERG1 currents, in the presence of MMS, an  $E_m$  value of  $-60.0 \pm 2.5$  mV ( $n=7$ ) was observed, analogous to that measured in the untreated cells. Therefore, the

treatment with the genotoxic agent *per se* does not modify either the biophysical properties of the channels, or the basal membrane potential of the Kv11.1-expressing cells.

### **Effect of MMS on cell viability and colony forming efficiency.**

To study the possible differences in MMS sensitivity of the different cell lines, their cell viability was determined using the MTS assay (see Methods). The percentage of cell survival with different concentrations of the genotoxic agent was determined 24 h after the 3 h MMS treatment, because no effect was detected when measurements were performed immediately after treatment. The results obtained for HEK293, H36 and T2 cells are presented in Figure 3A. As observed, the presence of MMS caused a progressive decrease of cell viability, that in all cases became particularly intense at the three highest analysed concentrations. Nevertheless, viability always remained above 50% except at the two highest MMS concentrations (0.5 and 0.6 mM), depending on the cell lines. Statistical analysis of cell survival within each cell line, when those cells treated with different MMS concentrations were compared to their respective negative controls (untreated cells), demonstrated that in H36 cells statistically significant decreases in viability started at 0.025 mM. In contrast, concentrations of at least 0.15 and 0.5 mM MMS were necessary to cause a significant decrease of viability in T2 and HEK293 cells, respectively. Furthermore, comparison of variations between different cell lines indicated that, except for the two highest concentrations tested (0.5 and 0.6 mM), the survival of both HEK293 and T2 cells were clearly higher than that of H36 cells at concentrations above 0.05 mM. Strikingly, a higher viability was observed in H36 ( $56.7 \pm 2.5\%$ ,  $n=6$ ) when compared to HEK293 cells ( $45.3 \pm 4.3\%$ ,  $n=4$ ) at 0.5 mM MMS, a difference that disappeared at 0.6 mM of the genotoxic agent.

The use of a Probit analysis, to optimize the determination of the dose causing a 50% inhibition of cell survival (see Methods), yielded similar  $IC_{50}$  values of 527, 506 and 502  $\mu\text{M}$  for HEK293, H36 and T2 cell lines, respectively. When Hill models were fitted to the dose–response data of the individual experiments using the eeFit add-in for Microsoft Excel ([87], see Methods and Figure 3A), an  $IC_{50}$  of  $342 \pm 49 \mu\text{M}$  ( $n=6$ ) was obtained for H36 cells, slightly smaller than those for HEK293 [ $490 \pm 24 \mu\text{M}$  ( $n=4$ )] and T2 cells [ $469 \pm 32 \mu\text{M}$  ( $n=9$ )], although these differences were not statistically significant. Considering all these data, MMS concentrations of 0.05, 0.1, 0.2 and 0.35 mM, all of them well above 50% of cell survival, and MMS treatment times of 3 h, were chosen to be used in subsequent studies of clonogenicity, apoptosis, cell cycle progression and induced DNA damage to check genomic instability. Since the highest concentration in this range was

similar to those used when MMS was employed as positive control in the comet assay [23], no additional positive controls were included in those experiments. Altogether, our results indicated that the presence of Kv11.1 was able to sensitize H36 cells to low and medium MMS concentrations.

To evaluate the cytotoxicity of MMS on cells expressing Kv11.1, results obtained with the colony formation assay in H36 cells were compared with those obtained in control HEK293 cells (Figure 3B). The number of cell colonies formed indicated that the genotoxic agent did not have cytotoxic effect on H36 cells in concentrations below 0.35 mM. However, contrary to the viability data, a slightly higher sensitivity was observed in HEK293 cells, compared to H36 cells, because a significant decrease of formed cell colony was also detected at 0.2 mM MMS.

### **Influence of Kv11.1 expression on MMS-induced DNA damage.**

To check the influence of the presence of Kv11.1 on the induction of DNA damage by MMS, we performed direct measurements of DNA damage using the Comet assay under alkaline conditions (see Methods), and measuring the percentage of DNA in the tail (% Tail DNA), which in mammalian cells constitutes the usual and recommended parameter to quantify DNA damage [15]. Again, measurements of MMS-induced DNA damage were performed with HEK293, H36 and T2 cell lines and the results obtained are depicted in Figure 4. As expected, dose-response regression analysis demonstrated that in every cell type, the DNA damage was significantly enhanced in response to increasing MMS concentrations, since positive slopes of the dose-response relationships statistically different from zero were obtained [76.1 ( $p=0.005$ ), 50.1 ( $p=0.008$ ), and 71.6 ( $p=0.004$ ), for HEK293, H36 and T2 cells, respectively]. No differences in spontaneous DNA damage were detected among the cell lines. However, when 0.2 mM MMS-induced DNA damage was compared with one-way ANOVA and SNK post-hoc tests, the damage was lower in H36 than in HEK293 and T2 cells (Figure 4), and the same was also true for 0.1 and 0.35 mM MMS concentrations. These results indicated that, at MMS concentrations higher than 0.1 mM, the presence of Kv11.1, but not the transfection routine alone, was able to protect the cells from the MMS-induced DNA damage.

### **Influence of Kv11.1 expression on cell apoptosis in response to MMS treatment.**

The percentage of apoptotic cells in the three cell lines was determined by flow cytometry, using the Annexin V-FITC plus PI assay. Early apoptotic cells are characterized by the presence of changes such as the redistribution of phosphatidylserine from the inner

to the outer plasma membrane leaflets [22]. Due to the ability of annexin V to interact with the phospholipid, the use of this protein labelled with a fluorescent marker, such as fluorescein isothiocyanate (FITC), constitutes a tool to specifically determine early apoptosis levels [75]. On the other hand, additional dysfunctions and morphologic changes are typically found in late apoptotic cells, including loss of cell membrane integrity [22]. This allows the fluorescent intercalating agent propidium iodide (PI) to enter the cells and stain them upon binding to DNA [75]. Therefore, data from flow cytometry assays with cells exposed to annexin V-FITC plus PI, in which only annexin V stained cells are detected, were considered as due to early apoptosis. Alternatively, those cells also stained with PI were considered as late apoptotic cells. The effect of treatment with different MMS concentrations on HEK293, H36 and T2 cells early and late apoptosis is depicted in Figure 5.

Analysis of early apoptosis showed that, although there were some increments induced by MMS treatments in the three cell lines, no statistically significant differences were found. Regarding late apoptosis, only 0.35 mM MMS induced a significant increase, compared to the respective negative controls, in T2 cells. However, the dose-response regression analyses showed that in H36 and T2 cells late apoptosis was progressively enhanced when MMS concentrations were increased (slopes, significantly different from zero, were  $1.44 \pm 0.43$ ,  $p= 0.042$ , and  $2.71 \pm 0.83$ ,  $p= 0.045$ , for H36 and T2, respectively).

These results showed that, since there were not significant differences between H36 cells, expressing the channel, and the parental HEK293 cells, or between H36 and T2 cells in the regression analyses, the presence of Kv11.1 did not seem to influence MMS-induced apoptosis.

### **Influence of Kv11.1 expression on cell cycle progression.**

Using flow cytometry, we studied cell cycle progression in the three analysed cell lines, to check the possible influence of Kv11.1 expression on the response to MMS exposition, following a 3 h treatment with the agent. As with the viability and apoptosis, cell cycle progression was determined 24 h after MMS treatment, because no effects were detected when measured immediately after treatment. Due to differences in DNA amount during cell cycle G1, S and G2 phases, it is possible to estimate the percentage of cells in every phase after incubating them with PI. The results of the cell cycle analysis are summarized in Figure 6. In the negative controls, without MMS, the three tested cell lines presented over 50% of cells in G1, and below 25% in G2. In this case, only a significantly lower percentage of H36 cells in G1 respect to the other two cell lines ( $p= 0.0084$ , one-way

ANOVA and SNK post-hoc tests), and a higher percentage H36 in S phase respect to HEK293 ( $p=0.01$  with Student's  $t$  test) were detected. On the other hand, in the presence of MMS, the percentage of cells in G1 remained almost unaltered at low concentrations of the agent in all cell lines, but was similarly lowered both in H36 and T2 cells at 0.2 mM, and appeared drastically decreased in the three cell lines at the highest (0.35 mM) tested concentration. Concomitantly, clear increases in G2 cells were also detected at these highest concentrations, but again, no differences were detected between the H36 cells expressing Kv11.1 and the T2 used as transfection control, in which the channel is absent (lower panels in Fig. 6). Finally, significant but almost identical increases of cells in S phase were observed at 0.35 mM MMS both in the H36 and the T2 cell lines. Again, like mentioned above with the apoptosis analysis, and shall be discussed below, the absence of any detectable difference between H36 and T2 seemed to indicate that, in terms of cell cycle progression, the expression of Kv11.1 does not influence the response to the DNA damaging agent MMS.

### **Canonical ion flux-dependent channel function is necessary for Kv11.1 modulation of MMS-induced changes of cell viability and DNA damage.**

To check if the Kv11.1-dependent modification of MMS-induced DNA damage needed  $K^+$  ion fluxes, channel-expressing H36 cells were treated with the specific erg channels blocker E4031. As an initial step to this end, we tested the efficiency of the treatment with the channel inhibitor by recording Kv11.1 currents in cells incubated with E4031 (see Methods). For this purpose, we electrophysiologically checked the Kv11.1 blocking ability of E4031 under basal conditions, without modification of the cell membrane potential, and also after depolarizing the membrane either applying depolarization pulses under voltage-clamp conditions, or chemically depolarizing it using a high extracellular  $K^+$  concentration.

Astonishingly, long treatments with 5  $\mu$ M E4031, up to 24 h, did not completely block the Kv11.1 currents, if current magnitudes were quantified during the first depolarization sequence, after completion of perforated-patch electrical access to the cell inside (Figure 7A,C). Indeed, the incomplete blockade of the currents was not due to an excessively low concentration of the inhibitor, since the currents were abolished after repeatedly applying depolarization steps at 20 s intervals (Figure 7B). Moreover, no Kv11.1 currents were observed when the first recording was preceded by a 30 s depolarization to 0 mV under voltage-clamp, or when the 3 h incubation period with 5  $\mu$ M E4031 in standard culture medium, was preceded by 5 min exposition to the inhibitor in a depolarizing saline

containing 140 mM KCl (Figure 7A,C). These data demonstrated that, unless the cells were briefly depolarized, either electrophysiologically or by chemically collapsing the transmembrane  $K^+$  gradient for a short period of time in the presence of the inhibitor, a complete blockade of the Kv11.1 currents was not achieved in H36 cells.

Having demonstrated the technical conditions in which a complete blockade of the Kv11.1 channel activity could be achieved, E4031 was used as a tool to test the contribution of the canonical ion flux-dependent hERG1 function to MMS-induced changes in cell viability and DNA damage. As shown in Figure 8A, at intermediate MMS concentrations the percent of viable H36 cells treated with the inhibitor were considerably higher than that of cells non treated with E4031. Indeed, at all concentrations tested, the viabilities of H36 cells treated with E4031 became almost identical to those of T2 cells, that do not express the channel.

With respect to the effect of E4031 on the Kv11.1 modulation of MMS-induced DNA damage (Figure 8B), the obtained results indicated that, providing that a complete blockade of Kv11.1 currents was ensured by means of a short preincubation with E4031 in depolarizing high-K saline, before the co-treatment with the inhibitor and the genotoxic agent, MMS-induced DNA damage in H36 cells was clearly higher than that detected when hERG1 current was not inhibited, whereas there was no E4031 effect in the case of T2 cells. Indeed, under these complete current blocking conditions, no significant differences of induced % Tail DNA were observed between E4031-treated H36 and T2 cells (Figure 8B). Noticeably, when the inhibitor was used without the depolarizing incubation period, only a slight but non-significant increase of induced DNA damage was detected in H36 cells incubated with E-4031, as compared with the untreated cells (see inset in Figure 8B). It is interesting to note also that this very small effect is observed in spite of the fact that, under these conditions in which a partial blockade of the currents is achieved, a significant drop in the basal membrane potential was just observed (see Figure 2), that remained still more negative than the  $E_m$  of the HEK293 cells, but become similar to that recorded in the T2 cells, because probably the dominance of the endogenous cell conductances setting  $E_m$  has been restored. This suggests that although part of the Kv11.1 modulation of DNA damage may be indirectly exerted through modifications in cell membrane potential, a complete blockade of  $K^+$  permeation itself seems fundamental for a more extensive protection against the MMS-induced DNA damage. In any case, our results indicate that the effects of Kv11.1 expression on the response to MMS, in terms of cell viability and DNA damage, were dependent on the canonical ion-conducting property of the channel.

## **Is Kv11.1 modulation of MMS-induced changes on DNA damage related to DNA repair?**

To study whether Kv11.1 expression effect in MMS-induced DNA damage was related to DNA repair, two types of experiments were carried out with HEK293 and H36 cells. First of all, the Comet assay was performed at different times after the end of the treatment, to check the disappearance of the induced DNA damage with time. As observed in Figure 9A, the DNA damage induced by 0.2 mM MMS started decreasing 1 h after the end of MMS treatment in HEK293 cells. However, the considerably lower induced DNA damage in H36 cells as compared to that in HEK293 cells (see also above), was not decreased in H36 cells, even 2 h after finishing the MMS treatment. So, apparently, some DNA repair activity damage removal was detected in HEK293 cells but not in H36 cells, at least within 2 h after removal of MMS.

Secondly, the expression of the *PARP1* gene in HEK293 and H36 cells, untreated and treated with 0.2 mM MMS, was studied by qPCR, using the *GAPDH* gene as reference [68]. The results presented in Figure 9B indicated that in untreated cells the expression level of *PARP1* in H36 cells is clearly higher (almost doubled) than that observed in HEK293 cells. On the other hand, after MMS treatment, whereas *PARP1* expression in HEK293 cells slightly increased, it clearly decreased in H36 cells.

## **DISCUSSION**

In this report, we have checked the possible influence of Kv11.1 on the DNA damage response induced by treatments with the genotoxic agent MMS. We have studied this response analysing viability, clonogenic efficiency, cell cycle progression, apoptosis and DNA damage as indicators of genomic instability induction in HEK293 cells permanently expressing the channel (H36), in the parental cells lacking the channel protein, and also in a second transfected cell line (T2, used as transfection control). Furthermore, the contribution of the potassium ion permeation function to the Kv11.1-dependent modifications of cell viability and induced DNA damage was studied employing as a tool the erg channels specific inhibitor E4031.

In agreement with previous information about MMS, in this work we have found that 3 hours treatments with this genotoxic chemical decreased cell viability with increasing concentrations, decreased clonogenic efficiency, induced arrest of cell cycle at G2 and S phases, and induced DNA damage, detected as DNA strand breaks. When these results were compared to those previously published on the MMS effects, we found that, with

respect to viability, HEK293 cells seemed to be more sensitive than others, like cervical carcinoma HeLa, non-small cell lung cancer H1299, hepatoma Hep3B or fibrosarcoma HT1080 cells, because equivalent decreases in cell viability were obtained in those cells with similar MMS concentrations but with considerably longer treatment times [14,29,43]. With respect to clonogenic efficiency, the decrease in clone formation observed after MMS treatment also agreed with those described with similar concentration but longer treatments [45].

Considering apoptosis, it has been shown that MMS induced apoptosis, both through p53-dependent and -independent mechanisms [44,76], when MMS concentrations higher than 0.2 mM and treatment times of at least 12 hours were used [14,29,43,84]. The small induction of late apoptosis induced by MMS here in T2 cells, and only suggested in H36 cells with regression analyses, does not disagree with those data because the MMS dose used in this work was considerably lower than those used by other authors.

With respect to cell cycle progression analysis, generation of DNA damage triggers cell responses that can be related to regulation of cell cycle progression [78]. Thus, in the presence of genotoxic injury, cell cycle checkpoints are used to promote cell survival by causing cell cycle arrest to give enough time to repair the damage. Due to induction of several types of DNA damage, including replication-blocking DNA adducts and AP sites, and the subsequent single strand DNA breaks, at relatively high concentrations MMS is able to induce cell cycle arrest in G2 phase and, mostly in S phase [70,78]. In our work, 200 and 350  $\mu$ M MMS induced cell cycle arrests in G2 and S phases, as described in other cell types with similar concentrations and longer treatment times [14,29,43,84].

Finally, MMS-induced DNA damage in HEK293 cells, detected with the comet assay, was similar to that induced in A549 cells under similar treatment conditions [23]. Other works determining MMS-induced DNA damage with the comet or micronuclei assays, or checking the number of  $\gamma$ -H2AX foci, showed induction of DNA damage at concentrations above 0.05 mM, although most of these effects were determined with longer treatment times, and depended on the cell type [14,29,34,43,84].

According to this information, MMS was working as expected, and the possible effect of the Kv11.1 channel expression on the cell response to this chemical could be analysed.

First of all, when analysing the MMS-induced apoptosis, the fact that no differences were found between H36 and HEK293 cells, and that the suggested increase detected with regression analysis in H36 cells was also found in T2 cells, seemed to suggest that the presence of Kv11.1 was not playing any role in this response. A relationship between hERG1 and apoptosis has been proposed [7,40,73], mostly indicating a pro-apoptotic effect of hERG1 inhibitors or hERG1 silencing [40,93], but also suggesting an anti-apoptotic

effect of such inhibitors in response to DNA damaging agents such as cisplatin or hydrogen peroxide [88,93]. Our results, with no effects of Kv11.1 on MMS response, might be possibly due to the lack of apoptosis response induced by MMS treatment.

When analysing the possible effects of Kv11.1 on the progression of cell cycle, our results showed that the percentage of H36 non-treated cells in G1 phase was lower than those of non-treated HEK293 and T2 cells, as recently described for hERG1-expressing human chronic myeloid leukemia (CML) cells when compared with cells treated with E4031 [77]. Analysing the influence of Kv11.1 expression on MMS induced changes on cell cycle progression, we detected MMS-induced increases in G2 and S phases in cells expressing the channel, as described before for cells treated with ionizing radiation [67]. However, since no differences between H36 and T2 cells were detected, the presence of Kv11.1 does not seem to be the crucial factor involved in the MMS-induced modifications of the cell cycle.

Contrary to these results on apoptosis and cell cycle progression, the presence of Kv11.1 influenced MMS-induced effects on cell viability, clonogenic efficiency and DNA damage.

With respect to cell viability, some effects favouring cell progression were already described for this channel in colon cancer cell lines [53,72], leukemia [71], melanoma [1], and also in HEK293 cells transfected with hERG1 [1]. In our case, we detected clear effects of Kv11.1 expression, increasing the sensitivity of MMS-treated cells. Our results, especially at low/medium doses, were equivalent to those obtained in gastric cancer cells treated with cisplatin, because in that case cells not expressing Kv11.1 were less sensitive than those expressing the channel [93]. These results are also equivalent to those obtained with cells after treatment with H<sub>2</sub>O<sub>2</sub>, because the cells expressing hERG1 were more sensitive to the chemical than those not expressing the channel [88].

However, our viability data differed from the clonogenic efficiency ones, showing that HEK293 cells seemed to be slightly more sensitive than the cells expressing Kv11.1 channels. These clonogenic efficiency data agreed with those obtained with CML K562 cells treated with ionizing radiation, indicating that exposed cells without hERG1 were more sensitive than cells expressing the channel [67]. We do not presently know the reasons for the apparent discrepancy between these two set of results. However, although related, both assays measure different, pleiotropic and perhaps cell-dependent phenomena, that may show quite complex relationships with the genotoxic agent-induced DNA damage level.

Considering DNA damage, expression of Kv11.1 protected against MMS-induced effects, because the detected damage levels were lower in H36 than in those cells not expressing the channel. These results are the first evidence that the presence of Kv11.1

could protect cells against the induction of DNA damage. They are further supported by the fact that the amount of DNA damage detected in both HEK293 (33.4%) and T2 cells (30.4%) with 0.35 mM MMS, was analogous to that previously described (32.0%), when a similar 3 h treatment with 0.3 mM of the chemical was performed in A549 lung adenocarcinoma cells [23], that exhibit very low levels of hERG1 expression [13,88]. Our data also resembled those obtained with CML K562 cells treated with ionizing radiation, in which DNA damage estimations measuring residual  $\gamma$ -H2AX foci seemed to be higher in cells not expressing the channel, although differences with cells expressing it were not statistically significant [67]. Although this lower induced DNA damage in H36, compared to T2 cells, might explain differences in apoptosis between these two cell types, at this point, it would be tempting to argue that these data on DNA damage contradict the results of cell cycle progression in which no differences were found between H36 and T2 cells. However, it is necessary to consider that although the presence of Kv11.1 decreased the induced DNA damage, it did not abolish it. Thus, it is possible to speculate that in H36 cells, the level of MMS-induced DNA damage was still high enough to influence this response to some extent similar to that observed in the T2 cells. In any case, our results point out the convenience of performing direct DNA damage determinations (e.g. through quantification of comet assay data as depicted here), in addition to other more usually analysed parameter, to obtain more reliable conclusions about the effect of Kv11.1 on DNA damage levels.

In this work, the detected effects of Kv11.1 expression in MMS-induced cell viability changes and DNA damage were related to the  $K^+$ -permeation of the channel, since they were reverted when the Kv11.1 ion current was inhibited with E4031. It is interesting to note that the relevance of this conductive function, not only for proper maintenance of cell electrogenesis and membrane potential, but also favouring several aspects related to tumour progression, has been previously highlighted according to data obtained in the presence not only of E4031, but also of other erg channels inhibitors [1,3,53,56,71,72].

It has been reported that efficient blockade of Kv11.1 channels with E4031 can be achieved at nanomolar concentrations [49,83,92,94]. However, for the DNA damage studies we choose to treat the cells with a relatively high amount of the compound, due to its known ability to interact with serum proteins of the culture medium [30,57], which might lead to a reduction of its effective concentration, as compared to the levels acting on patch-clamp recordings in which the potency of the inhibition has to be evaluated in serum-free extracellular saline. Moreover, the inhibitory effect of E4031 is use-dependent, since its interaction with the binding site behind the cytoplasmic channel gate is favoured by channel opening [81,83]. Thus, in the non-excitable HEK cells, with a relatively constant

transmembrane potential that can be maintained during long periods of time, it is necessary to depolarize the cells to be sure that the inhibitor works. This necessity is particularly relevant for cells such as H36, showing quite negative membrane potential values, probably due to the over-expression of Kv11.1. Indeed, since it was necessary to depolarize the cell during the first voltage steps to measure the currents, the real steady inhibition before the initial recording should be still lower than that showed in the graphs presented here. Therefore, our results emphasize the relevance of performing proper controls to ensure that the sought channel inhibition is complete, to be sure that reliable conclusions are obtained about the involvement of Kv11.1 canonical functions. This will be particularly relevant for cells lacking intrinsic electrical activity, such as most tumour cells. Interestingly, the significant differences encountered when a short 5 min depolarization was performed, to ensure an effective channel blockade, seemed to exclude the possibility that the E4031 actions were due to other side effects of the chemical during long-term exposure of the cells, such as modifications of protein synthesis or trafficking. The use of additional cell lines carrying mutant Kv11.1 channels, exhibiting different conductive and gating properties (e.g. see [8]), might add further insights about this issue. Note also that whether the canonical influence demonstrated here was exerted directly through variations of the  $K^+$  flux and/or concentrations, by an indirect effect due to alterations in basal membrane potential, or through a combination of both, remains to be determined.

In our knowledge, this is the first time in which an effect of Kv11.1 expression on DNA damage induced by a specific genotoxic agent and measured through a direct estimation of the induced damage was demonstrated. The impact of the channel presence in cell response(s) associated to DNA damage induced by MMS seemed to take place at two levels. First, it enhanced MMS-induced mortality at small concentrations of the agent in a  $K^+$ -permeation dependent way. Interestingly, however, no significant differences in  $IC_{50}$  values were observed when the different cell lines were compared and, furthermore, the presence of the channel seemed to increase the clonogenic efficiency. Additional studies will be necessary to fully understand the reasons for this apparent discrepancy. Second, and perhaps more importantly, the presence of Kv11.1 lowered the MMS-induced DNA damage level. This effect was particularly evident at the highest MMS analysed concentrations, and also took place via a  $K^+$ -conductive dependent mechanism.

Since the extent of DNA damage is the result of a balance between two antagonistic processes, the induction of DNA damage caused by the genotoxic agent, and the efficiency of DNA damage repair systems [23], we tried to check if DNA repair activity might be different depending on the presence of the Kv11.1 channel. The performance of the Comet assay at different times after treatment allows the analysis of DNA damage removal

[58,66], and the obtained results suggest that whereas there was some repair activity in cells lacking the channel, there was no evidence of such activity in H36 cells, at least in 2 h after treatment. Although the possibility of a slower removal of intracellular MMS in H36 cells cannot be completely excluded, this result would be consistent with a decrease in DNA repair activity in these cells. However, such decrease seemed to be in contradiction with the fact that in H36 cells the MMS-induced DNA damage was lower than in HEK293 cells. Thus, it is tempting to speculate that an exclusive effect in DNA repair activity was not involved, since no differences in basal DNA damage were detected among cell lines, and all of them seemed to be similarly sensitive to MMS. Nevertheless, trying to get more information, we have studied expression of the *PARP1* gene, which encodes a protein involved in several DNA repair systems [74], including those that repair MMS-induced damage [38]. In fact, exposure to MMS activates the PARP1 protein [41,85]. Comparison of *PARP1* gene expression between untreated HEK293 and H36 cells revealed a higher expression on H36 cells, that might be at least partially responsible for the lower DNA damage induced by MMS in these cells. However, after treatment, whereas *PARP1* expression slightly increased in HEK293 cells [41], it clearly decreased in H36 cells. This might explain the lack of DNA damage removal detected with the comet assay after treatment. According to these results, it seems that the presence of Kv11.1 channels affects *PARP1* expression, before and after exposure to a genotoxic agent and, therefore might be influencing DNA repair activity. Since this is the first evidence of this influence, more studies would be necessary for confirmation. In any case, an effect of Kv11.1 on MMS activity, such as for instance slowing the induction of DNA damage and displacing the balance between DNA damage induction and repair, cannot be excluded with our data.

Apart from being the first time that an influence of Kv11.1 is directly demonstrated in the induction of DNA damage, it seems interesting to consider the possibility that this effect of the channel could be related to its recognized involvement in cell proliferation and/or tumour progression [8,17,47,62,64]. It would be important to know also if the impact of Kv11.1 expression could be confirmed for other cells and other types of DNA damage, due to the increased expression of this channel protein in a number of tumour cell types. Thus, possible limitations of our study concerned the use of HEK293 cells, a cell line immortalized by adenovirus infection that is not of cancer origin [31,35,42,48], and employing cell lines heterologously overexpressing Kv11.1.

In any case, our data may be important to better understand, not only the possible impact of hERG1 channels in several aspects of tumour progression [25,69,73], but also its possible negative effect in the response to some tumour therapies [39], if the presence of

the channel is able to limit the level of DNA damage induced by some antitumoral agents, as demonstrated here.

## REFERENCES

1. Afrasiabi E, Hietamäki M, Viitanen T, Sukumaran P, Bergelin N, Törnquist K (2010) Expression and significance of HERG (KCNH2) potassium channels in the regulation of MDA-MB-435S melanoma cell proliferation and migration. *Cell Signal* 22:57–64. doi: 10.1016/j.cellsig.2009.09.010
2. Arcangeli A, Becchetti A (2016) hERG channels: From antitargets to novel targets for cancer therapy. *Clin Cancer Res* 23:3-5. doi: 10.1158/1078-0432
3. Arcangeli A, Crociani O, Lastraioli, Masi EA, Pillozzi S, Becchetti A (2009) Targeting ion channels in cancer: A novel frontier in antineoplastic therapy. *Curr Med Chem* 16:66-93. doi: 10.2174/092986709787002835
4. Azqueta A, Ladeira C, Giovannelli L, Boutet-Robinet E, Bonassi S, Nerig M, Gajski G, Duthie S, Del Bo C, Riso P, Koppen G, Basaran N, Collins A, Møller P (2020) Application of the comet assay in human biomonitoring: An hCOMET perspective. *Mutat Res* 783:108288. doi: 10.1016/j.mrrev.2019.108288
5. Barros F, de la Peña P, Domínguez , Sierra, LM, Pardo LA (2020) The EAG voltage-Dependent K<sup>+</sup> channel subfamily: Similarities and differences in structural organization and gating. *Front Pharmacol* 11:411. doi: 10.3389/fphar.2020.00411
6. Barros F, Pardo LA, Domínguez , Sierra, LM, de la Peña P (2019). New structures and gating of voltage-dependent potassium (Kv) channels and their relatives: A multi-domain and dynamic question. *Int J Mol Sci* 20:248. doi: 10.3390/ijms20020248
7. Becchetti A (2011) Ion channels and transporters in cancer. 1. Ion channels and cell proliferation in cancer. *Am J Physiol Cell Physiol* 301:C255-C265. doi: 10.1152/ajpcell.00047.2011
8. Becchetti A, Crescioli S, Zanieri F, Petroni G, Mercatelli R, Coppola S, Gasparoli L, D'Amico M, Pillozzi S, Crociani O, Stefanini M, Fiore A, Carraresi L, Morello V, Manoli S, Brizzi MF, Ricci D, Rinaldi M, Masi A, Schmidt T, Quercioli F, Defilippi P, Arcangeli A (2017) The conformational state of hERG1 channels determines integrin association, downstream signaling, and cancer progression. *Sci Signal* 10:eaaf3236. doi: 10.1126/scisignal.aaf3236
9. Beranek DT (1990) Distribution of methyl and ethyl adducts following alkylation with monofunctional alkylating agents. *Mutat Res* 231:11-30. doi: 10.1016/0027-5107(90)90173-2
10. Bolognesi C, Cirillo S, Chipman JK (2019) Comet assay in ecogenotoxicology: Applications in *Mytilus* sp. *Mutat Res* 842:50-59. doi: 10.1016/j.mrgentox.2019.05.004
11. Brackenbury WJ (2016) Ion Channels in Cancer. In: *Ion Channels in Health and Disease*. Pitt G (ed) Health and Disease, 1st edn. Academic Press, pp. 131-163. doi: 10.1016/B978-0-12-802002-9.00006-6
12. Carretero L, Barros F, Miranda M, Fernández-Trillo J, Machín A, de la Peña P, Domínguez P (2012) Cell type influences the molecular mechanisms involved in hormonal regulation of ERG K<sup>+</sup> channels. *Pflugers Arch - Eur J Physiol* 463:685–702. doi: 10.1007/s00424-012-1094-y
13. Chen SZ, Jiang M, Zhen YS (2005) HERG K<sup>+</sup> channel expression-related chemosensitivity in cancer cells and its modulation by erythromycin. *Cancer Chemother Pharmacol* 56:212-220. doi: 10.1007/s00280-004-0960-5
14. Clewell RA, Sun B, Adeleye Y, Carmichael P, Efremenko A, McMullen PD, Pendse S, Trask OJ, White A, Andersen ME (2014) Profiling Dose-Dependent Activation of p53-Mediated Signaling Pathways by Chemicals with Distinct Mechanisms of DNA Damage. *Toxicol Sci* 142:2014, 56–73. doi: 10.1093/toxsci/kfu153
15. Collins AR (2004) The comet assay for DNA damage and repair: principles, applications, and limitations. *Mol Biotechnol* 26:249-261. doi: 10.1385/MB:26:3:249

16. Collins AR, Azqueta A, Brunborg G, Gaivão I, Giovannelli L, Kruszewski M, Smith CC, Stetina R (2008) The comet assay: topical issues. *Mutagenesis* 23:143-151. doi: 10.1093/mutage/gem051
17. Comes N, Serrano-Albarrás A, Capera J, Serrano-Novillo C, Condom E, Ramón y Cajal S, Ferreres JC, Felipe A (2015) Involvement of potassium channels in the progression of cancer to a more malignant phenotype. *Biochim Biophys Acta* 1848:2477–2492. doi: 10.1016/j.bbamem.2014.12.008
18. Crociani O, Zanieri F, Pillozzi S, Lastraioli E, Stefanini M, Fiore A, Fortunato A, D'Amico M, Masselli M, De Lorenzo E, Gasparoli L, Chiu M, Bussolati O, Becchetti A, Arcangeli A (2013) hERG1 channels modulate integrin signaling to trigger angiogenesis and tumor progression in colorectal cancer. *Sci Rep* 3:3308. doi: 10.1038/srep03308
19. de la Peña P, Delgado LM, del Camino D, Barros F (1992) Cloning and expression of the thyrotropin-releasing hormone receptor from GH<sub>3</sub> rat anterior pituitary cells. *Biochem J* 284:891-899. doi: 10.1042/bj2840891
20. Dhawan A, Bajpayee M, Parmar D (2009) Comet assay: a reliable tool for the assessment of DNA damage in different models. *Cell Biol Toxicol* 25:5-32. doi: 10.1007/s10565-008-9072-z
21. Downie BR, Sánchez A, Knötgen H, Contreras-Jurado C, Gymnopoulos M, Weber C, Stühmer W, Pardo LA (2008) Eag1 expression interferes with hypoxia homeostasis and induces angiogenesis in tumors. *J Biol Chem* 283:36234–36240. doi: 10.1074/jbc.M801830200
22. Elmore S (2007) Apoptosis: a review of programmed cell death. *Toxicol Pathol* 35:495-516. doi: 10.1080/01926230701320337
23. Espina M, Corte-Rodríguez M, Aguado L, Montes-Bayón M, Sierra MI, Martínez-Cambor P, Blanco-González E, Sierra LM (2017) Cisplatin resistance in cell models: evaluation of metallomic and biological predictive biomarkers to address early therapy failure. *Metallomics* 9:564. doi: 10.1039/c7mt00014f
24. Florea A-M, Büsselberg D (2009) Anti-cancer drugs interfere with intracellular calcium signaling. *NeuroToxicology* 30:803-810. doi: 10.1016/j.neuro.2009.04.014
25. Fraser SP, Pardo LA (2008) Colloquium on ion channels and cancer. *EMBO Rep* 9:512-515. doi: 10.1038/embor.2008.75
26. Gajski G, Zegurab B, Ladeira C, Novak M, Sramkova M, Pourrut B, Del Bo C, Milić M, Bjerve Gutzkow K, Costa S, Dusinska M, Brunborg G, Collins A (2019b) The comet assay in animal models: From bugs to whales – (Part 2 Vertebrates). *Mutat Res* 781:130-164. doi: 10.1016/j.mrrev.2019.04.002
27. Gajski G, Zegurab B, Ladeira C, Pourrut B, Del Bo C, Novak M, Sramkova M, Milić M, Bjerve Gutzkow K, Costa S, Dusinska M, Brunborg G, Collins A (2019a) The comet assay in animal models: From bugs to whales – (Part 1 Invertebrates). *Mutat Res* 779:82-113. doi: 10.1016/j.mrrev.2019.02.003
28. Gaivão I, Sierra LM (2014) Drosophila comet assay: insights, uses, and future perspectives. *Front Genet* 5:304. doi: 10.3389/fgene.2014.00304
29. Gao X, Zhang G, Shan S, Shang Y, Chi L, Li H, Cao Y, Zhu X, Zhang M, Yang J (2016) Depletion of paraspeckle protein 1 enhances methyl methanesulfonate-induced apoptosis through mitotic catastrophe. *PLoS ONE* 11: e0146952. doi: 10.1371/journal.pone.0146952
30. Glassmeier G, Hempel K, Wulfen I, Bauer CK, Schumacher U, Schwarz JR (2012) Inhibition of HERG1 K<sup>+</sup> channel protein expression decreases cell proliferation of human small cell lung cancer cells. *Pflugers Arch - Eur J Physiol* 463:365–376. doi: 10.1007/s00424-011-1045-z
31. Graham FL, Smiley J, Russell WC, Nairn R (1977) Characteristics of a human cell line transformed by DNA from human adenovirus type 5. *J. Gen Virol* 36:59-72. doi: 10.1099/0022-1317-36-1-59

32. Guidarelli A, Cattebeni F, Cantoni O (1997) Alternative mechanisms for hydroperoxide-induced DNA single strand breakage. *Free Rad Res* 26:537-547. doi: 10.3109/10715769709097825
33. Gutman GA, Chandy KG, Grissmer S, Lazdunski M, McKinnon D, Pardo LA, Robertson GA, Rudy B, Sanguinetti MC, Stühmer W, Wang X (2005) International Union of Pharmacology. LIII. Nomenclature and molecular relationships of voltage-gated potassium channels. *Pharmacol Rev* 57:473–508. doi:10. 1124/pr.57.4.10
34. Habas K, Najafzadeh M, Baumgartner A, Brinkworth MH, Anderson D (2017) An evaluation of DNA damage in human lymphocytes and sperm exposed to methyl methanesulfonate involving the regulation pathways associated with apoptosis. *Chemosphere* 185:709e716. doi: 10.1016/j.chemosphere.2017.06.014
35. Hamid T, Malik MT, Kakar SS (2005) Ectopic expression of PTTG1/securin promotes tumorigenesis in human embryonic kidney cells. *Mol Cancer* 4:3. doi: 10.1186/1476-4598-4-3
36. Hervé JC (2015) Membrane channels and transporters in cancers. *Biochim Biophys Acta* 1848:2473–2476. doi: 10.1016/j.bbamem.2015.06.017
37. Hille B (2001) Ion channels of excitable membranes. Sinauer Associates, Sunderland, MA.
38. Hombach-Klonisch S, Kalantari F, Medapati MR, Natarajan S, Krishnan SN, Kumar-Kanojia A, Thanasupawat T, Begum F, Xu FY, Hatch GM, Los M, Klonisch T (2019) HMGGA2 as a functional antagonist of PARP1 inhibitors in tumor cells. *Mol Oncol* 13:153-170. doi: 10.1002/1878-0261.12390
39. Iorio J, Lastraioli E, Tofani L, Petroni G, Antonuzzo L, Messerini L, Perrone G, Caputo D, Francesconi M, Amato MM, Cadei M, Arcangeli G, Villanacci V, Boni L, Coppola R, Di Costanzo F, Arcangeli A (2020) hERG1 and HIF-2 $\alpha$  Behave as Biomarkers of Positive Response to Bevacizumab in Metastatic Colorectal Cancer Patients. *Transl Oncol* 13:100740. doi: 10.1016/j.tranon.2020.01.001
40. Jehle J, Schweizer PA, KatusHA, Thomas D (2011) Novel roles for hERG K<sup>+</sup> channels in cell proliferation and apoptosis. *Cell Death Dis* 2:e193. doi:10.1038/cddis.2011.77
41. Jelezcova E, Trivedi RN, Wang XH, Tang JB, Brown AR, Goellner EM, Schamus S, Fornsgaglio JL, Sobol RW (2010) Parp1 activation in mouse embryonic fibroblasts promotes Pol beta-dependent cellular hypersensitivity to alkylation damage. *Mutat Res* 686:57-67. doi: 10.1016/j.mrfmmm.2010.01.016
42. Jespersen C, Soragni E, C. Chou J, Arora PS, Dervan PB, Gottesfeld JM (2012) Chromatin structure determines accessibility of a hairpin polyamide–chlorambucil conjugate at histone H4 genes in pancreatic cancer cells. *Bioorg Med Chem Lett* 22:4068–4071. doi: 10.1016/j.bmcl.2012.04.090
43. Jiang Y, Zhang X-Y, Sune L, Zhang G-L, Duerksen-Hughes P, Zhub X-Q, Yang J (2012) Methyl methanesulfonate induces apoptosis in p53-deficient H1299 and Hep3B cells through a caspase 2- and mitochondria-associated pathway. *Environ Toxicology Pharmacol* 34:694–704. doi: 10.1016/j.etap.2012.09.019
44. Jin S, Fan F, Fan W, Zhao H, Tong T, Blanck P, Alomo I, Rajasekaran B, Zhan Q (2001) Transcription factors Oct-1 and NF-YA regulate the p53-independent induction of the GADD45 following DNA damage. *Oncogene* 20:2683-90. doi: 10.1038/sj.onc.1204390
45. Johannessen TC, Prestegarden L, Grudic A, Hegi ME, Tysnes BB, Bjerkvig R (2013) The DNA repair protein ALKBH2 mediates temozolomide resistance in human glioblastoma cells. *Neuro Oncol* 15:269-78. doi: 10.1093/neuonc/nos301.
46. Kaczmarek LK (2006) Non-conducting functions of voltage-gated ion channels. *Nat Rev Neurosci* 7:761-771. doi: 10.1038/nrn1988
47. Kassie F1, Parzefall W, Knasmüller S (2000) Single cell gel electrophoresis assay: a new technique for human biomonitoring studies. *Mutat Res* 463:13-31. doi: 10.1016/s1383-5742(00)00041-7

48. Kavsan VM, Iershov AV, Balynska OV (2011) Immortalized cells and one oncogene in malignant transformation: Old insights on new explanation. *BMC Cell Biol* 12:23. doi: 10.1186/1471-2121-12-23
49. Kirsch GE, Trepakovaa ES, Brimecombe JC, Sidacha SS, Erickson HD, Kochana MC, Shyjkaa LM, LacerdaAE, Brown AM (2004) Variability in the measurement of hERG potassium channel inhibition: Effects of temperature and stimulus pattern. *J Pharmacol Toxicol Meth* 50: 93–101. doi: 10.1016/j.vascn.2004.06.003
50. Klungland A, Laake K, Hoff E, Seeberg E (1995) Spectrum of mutations induced by methyl and ethyl methanesulfonate at the *hprt* locus of normal and *tag* expressing Chinese hamster fibroblasts. *Carcinogenesis* 16:1281-1285. doi: 10.1093/carcin/16.6.1281
51. Köberle B, Röscheisen C, Helbig R, Speit G (1993) Molecular characterization of methyl methanesulphonate (MMS)-induced HPRT mutations in V79 cells. *Mutat Res* 301,65-71. doi: 10.1016/0165-7992(93)90058-4
52. Kunzelmann K (2005) Ion channels and cancer. *J Membr Biol* 205:159-173. doi: 10.1007/s00232-005-0781-4
53. Lastraioli E, Guasti L, Crociani O, Polvani S, Hofmann G, Witchel H, Bencini L, Calistri M, Messerini L, Scatizzi M, Moretti R, Wanke E, Olivotto M, Mugnai G, Arcangeli A (2004) *herg1* gene and HERG1 protein are overexpressed in colorectal cancers and regulate cell invasion of tumor cells. *Cancer Res* 64:606-611. doi: 10.1158/0008-5472.can-03-2360
54. Lastraioli E, Lottini T, Bencini L, Bernini M, Arcangeli A (2015) hERG1 potassium channels: Novel biomarkers in human solid cancers. *BioMed Res Int* 2015:896432. doi: 10.1155/2015/896432
55. Litan A, Langhans SA (2015) Cancer as a channelopathy: ion channels and pumps in tumor development and progression. *Front Cell Neurosci* 9:86. doi: 10.3389/fncel.2015.00086
56. Manoli S, Coppola S, Duranti C, Lulli M, Magni L, Kuppala N, Nielsen N, Schmidt T, Schwab A, Becchetti A, Arcangeli A (2019) The activity of Kv11.1 potassium channel modulates F-Actin organization during cell migration of pancreatic ductal adenocarcinoma cells. *Cancers* 11:135. doi: 10.3390/cancers11020135
57. Menéndez ST, Rodrigo JP, Alvarez-Teijeiro S, Villaronga MA, Allonca E, Vallina A, Astudillo A, Barros F, Suárez C, García-Pedrero JM (2012) Role of HERG1 potassium channel in both malignant transformation and disease progression in head and neck carcinomas. *Mod Pathol* 25:1069-1078. doi: 10.1038/modpathol.2012.63
58. Metral E, Bechetoille N, Demarne F, Damour O, Rachidi W(2018) Keratinocyte stem cells are more resistant to UVA radiation than their direct progeny. *PLoS One* 13:e0203863. doi: 10.1371/journal.pone.0203863
59. Miranda P, Giráldez T, de la Peña P, Manso DG, Alonso-Ron C, Gómez-Varela D, Domínguez P, Barros F (2005) Specificity of TRH receptor coupling to G-proteins for regulation of ERG K<sup>+</sup> channels in GH<sub>3</sub> rat anterior pituitary cells. *J Physiol* 566:717-731. doi: 10.1113/jphysiol.2005.085803
60. Miranda P, Manso DG, Barros F, Carretero L, Hughes TE, Alonso-Ron C, Domínguez P, de la Peña P (2008) FRET with multiply labeled HERG K<sup>+</sup> channels as a reporter of the in vivo coarse architecture of the cytoplasmic domains. *Biochim Biophys Acta* 1783:1681-1699. doi: 10.1016/j.bbamcr.2008.06.009
61. Møller P (2018) The comet assay: ready for 30 more years. *Mutagenesis* 33:1-7. doi: 10.1093/mutage/gex046
62. Monteith GR, Prevarskaya N, Roberts-Thomson SJ (2017) The calcium-cancer signalling nexus. *Nat Rev Cancer* 17:367-380. doi: 10.1038/nrc.2017.18
63. Nivard MJM, Pastink A, Vogel EW (1992) Molecular analysis of mutations induced in the *vermilion* gene of *Drosophila melanogaster* by methyl methanesulfonate. *Genetics* 131:673-682
64. Ouadid-Ahidouch H, Ahidouch A (2013) K<sup>+</sup> channels and cell cycle progression in tumor cells. *Front Physiol* 4:220. doi: 10.3389/fphys.2013.00220

65. Ouadid-Ahidouch H, Ahidouch A, Pardo LA (2016) Kv10.1 K<sup>+</sup> channel: from physiology to cancer. *Pflugers Arch - Eur J Physiol* 468:751–762. doi: 10.1007/s00424-015-1784-3
66. Palazzo RP, Jardim LB, Bacellar A, de Oliveira FR, Maraslis FT, Pereira CHJ, da Silva J, Maluf SW (2018) DNA damage and repair in individuals with ataxia-telangiectasia and their parents. *Mutat Res* 836:122-126. doi: 10.1016/j.mrgentox.2018.06.007
67. Palme D, Misovic M, Ganser K, Klumpp L, Salih HR, Zips D, Huber SM (2020) hERG K<sup>+</sup> channels promote survival of irradiated leukemia cells. *Front Pharmacol* 11:489. doi: 10.3389/fphar.2020.00489
68. Panina Y, Germond A, Masui S, Watanabe TM (2018) Validation of Common Housekeeping Genes as Reference for qPCR Gene Expression Analysis During iPSC Reprogramming Process. *Sci Rep* 8:8716. doi: 10.1038/s41598-018-26707-8
69. Pardo LA, Stühmer W (2014) The roles of K<sup>+</sup> channels in cancer. *Nat Rev Cancer* 14:39-48. doi: 10.1038/nrc3635
70. Paulovich AG, Hartwell LH (1995) A checkpoint regulates the rate of progression through S phase in *S. cerevisiae* in response to DNA damage. *Cell* 82:841-847. doi: 10.1016/0092-8674(95)90481-6
71. Pillozzi S, Brizzi MF, Balzi M, Crociani O, Cherubini A, Guasti L, Bartolozzi B, Becchetti A, Wanke E, Bernabei PA, Olivetto M, Pegoraro L, Arcangeli A (2002) HERG potassium channels are constitutively expressed in primary human acute myeloid leukemias and regulate cell proliferation of normal and leukemic hemopoietic progenitors. *Leukemia* 16:1791–1798. doi: 10.1038/sj.leu.2402572
72. Pillozzi S, D’Amico M, Bartoli G, Gasparoli L, Petroni G, Crociani O, Marzo M, Guerriero A, Messori L, Severi M, Udisti R, Wulff H, Chandry KG, Becchetti A, Arcangeli A (2018) The combined activation of KCa3.1 and inhibition of Kv11.1/hERG1 currents contribute to overcome Cisplatin resistance in colorectal cancer cells. *Br J Cancer* 118:200-212. doi:10.1038/bjc.2017.392
73. Prevarskaya N, Skryma R, Yaroslav Shuba Y (2018) ion channels in cancer: are cancer hallmarks oncochannelopathies? *Physiol Rev* 98:559-621. doi: 10.1152/physrev.00044.2016
74. Ray Chaudhuri A, Nussenzweig A (2017) The multifaceted roles of PARP1 in DNA repair and chromatin remodelling. *Nat Rev Mol Cell Biol* 18:610-621. doi: 10.1038/nrm.2017.53.
75. Rieger AM, Nelson KL, Konowalchuk JD, Barreda DR (2011) Modified annexin V/propidium iodide apoptosis assay for accurate assessment of cell death. *J Vis Exp* 24:2597. doi: 10.3791/2597
76. Sgagias MK, Wagner KU, Hamik B, Stoeger S, Spieker R, Huber LJ, Chodosh LA, Cowan KH (2004) Brca1-deficient murine mammary epithelial cells have increased sensitivity to CDDP and MMS. *Cell Cycle* 3:1451-1456. doi: 10.4161/cc.3.11.1211
77. Shieh C-C, Coghlan M, Sullivan JP, Gopalakrishnan M (2000) Potassium channels: Molecular defects, diseases, and therapeutic opportunities. *Pharmacol Rev* 52:557–593.
78. Siler J, Xia B, Wong C, Kath M, Bi X (2017) Cell cycle-dependent positive and negative functions of Fun30 chromatin remodeler in DNA damage response. *DNA Repair* 50:61-70. doi: 10.1016/j.dnarep.2016.12.009
79. Singh NP (2016) The comet assay: Reflections on its development, evolution and applications. *Mutat Res* 767:23-30. doi: 10.1016/j.mrrev.2015.05.004
80. Singh NP, McCoy MT, Tice RR, Schneider EL (1988) A simple technique for quantitation of low levels of DNA damage in individual cells. *Exp Cell Res* 175:184-191. doi: 10.1016/0014-4827(88)90265-0
81. Spector PS, Curran ME, Keating MT, Sanguinetti MC (1996a) Class III antiarrhythmic drugs block HERG, a human cardiac delayed rectifier K<sup>+</sup> channel. *Circ Res* 78:499-503. doi: 10.1161/01.RES.78.3.499
82. Spector PS, Curran ME, Zou A, Keating MT, Sanguinetti MC (1996b) Fast inactivation causes rectification of the IKr channel. *J Gen Physiol* 107:611-619. doi: 10.1085/jgp.107.5.611

83. Stork D, Timin EN, Berjukow S, Huber C, Hohaus A, Auer M, Hering S (2007) State dependent dissociation of HERG channel inhibitors. *Br J Pharmacol* 151:1368-1376. doi: 10.1038/sj.bjp.0707356
84. Sun B, Ross SM, Rowley S, Adeleye Y, Clewell RA (2017) Contribution of ATM and ATR kinase pathways to p53-mediated response in etoposide and methyl methanesulfonate induced DNA damage. *Environ Mol Mutagen* 58:72–83. doi: 10.1002/em.22070
85. Tsuda M, Cho K, Ooka M, Shimizu N, Watanabe R, Yasui A, Nakazawa Y, Ogi T, Harada H, Agama K, Nakamura J, Asada R, Fujiike H, Sakuma T, Yamamoto T, Murai J, Hiraoka M, Koike K, Pommier Y, Takeda S, Hirota K (2017) ALC1/CHD1L, a chromatin-remodeling enzyme, is required for efficient base excision repair. *PLoS One* 12:e0188320. doi: 10.1371/journal.pone.0188320
86. Vandenberg JI, Perry MD, Perrin MJ, Mann SA, Ke Y, Hill AP (2012) hERG K<sup>+</sup> channels: Structure, function, and clinical significance. *Physiol Rev* 92:1393-1478. doi: 10.1152/physrev.00036.2011
87. Vivaudou M (2019) eeFit: a Microsoft Excel-embedded program for interactive analysis and fitting of experimental dose-response data. *BioTechniques* 66:186-193. doi: 10.2144/btn-2018-0136
88. Wang H, Zhang Y, Cao L, Han H, Wang J, Yang B, Nattel S, Wang Z (2002) HERG K<sup>+</sup> channel, a regulator of tumor cell apoptosis and proliferation. *Cancer Res* 62:4843– 4848
89. Wang Z (2004) Roles of K<sup>+</sup> channels in regulating tumour cell proliferation and apoptosis. *Pflugers Arch - Eur J Physiol* 448:274-286. doi: 10.1007/s00424-004-1258-5
90. Wulff H, Neil A, Castle NA, Pardo LA (2009) Voltage-gated potassium channels as therapeutic targets. *Nat Rev Drug Discov* 8:982-1001. doi: 10.1038/nrd2983
91. Yang M, Brackenbury WJ (2013) Membrane potential and cancer progression. *Front Physiol* 4:185. doi: 10.3389/fphys.2013.00185
92. Yao J-A, Du X, Lu D, Baker RL, Daharsh E, Atterson P (2005) Estimation of potency of HERG channel blockers: Impact of voltage protocol and temperature. *J Pharmacol Toxicol Meth* 52:146-153. doi: 10.1016/j.vascn.2005.04.008
93. Zhang R, Tian P, Chi, Wang J, Wang Y, Sun L, Liu Y, Tian S, Zhang Q (2012) Human ether-à-go-go-related gene expression is essential for cisplatin to induce apoptosis in human gastric cancer. *Oncol Rep* 27:433-440. doi: 10.3892/or.2011.1515
94. Zhou Z, Gong Q, Ye B, Fan Z, Makielski JC, Robertson GA, January CT (1998) Properties of HERG channels stably expressed in HEK 293 cells studied at physiological temperature *Biophys J* 74:230-241. doi: 10.1016/S0006-3495(98)77782-3

## FIGURE LEGENDS

**Figure 1.** Morphological and electrophysiological characterization of HEK293, H36 and T2 cells. **A** Bright field microscopy images of the different cell types in culture. **B** Comparison of depolarization-induced voltage-dependent ionic currents. Representative families of currents from the three cell types were recorded under voltage-clamp conditions in response to the voltage protocol represented on top of the HEK293 current traces. Currents from HEK293, H36 and T2 cells are shown at the top. Averaged I versus V relationships from H36 cells are shown at the bottom. A plot of normalized current magnitudes measured at the end of the depolarization steps (open circle above the current traces of the upper H36 panel) is shown on the left. A plot of normalized peak tail current magnitudes (black circle in the upper H36 currents panel) as a function of depolarizing voltage is represented on the right. The continuous line is a Boltzmann fit to the data as indicated in "Material and Methods" section, with a half point value ( $V_{0,5}$ ) at  $-11 \pm 1,5$  mV ( $n=7$ ). **C** Insensitivity of Kv11.1 current to treatment of H36 cells with 0.35 mM MMS. Two representative families of currents from one untreated control cell (Control), and from the same cell following a 5 min treatment with MMS directly perfused to the recording chamber (0.35 mM MMS) are shown on the upper left. A third current family from a cell submitted to a previous 3 h treatment with the genotoxic agent at 37°C in culture medium (marked 3h MMS 0.35 mM) is shown in the upper right panel. A plot of normalized peak tail current magnitudes as a function of depolarizing voltage is represented on the lower left.  $V_{0,5}$  values corresponded to  $14.5 \pm 1.6$  mV ( $n=4$ ),  $-15.2 \pm 2.1$  mV ( $n=4$ ) and  $-14.6 \pm 3.2$  mV ( $n=6$ ) for untreated controls, 0.35 mM MMS in perfusion, and 3h MMS 0.35 mM cells, respectively. A bar plot of averaged Kv11.1 tail current density (pA of peak tail current normalized to cell membrane area estimated as pF of cell capacitance) in untreated controls, cells treated for 5 min perfusing 0.35 mM MMS (MMS), and cells treated for 3h with the agent as indicated above (3h MMS), is shown at the bottom right.

**Figure 2.** Determination of resting membrane potential of HEK293, H36 and T2 cells, and effect of the Kv11.1 inhibitor E4031 on the treatment of H36 cells. Basal membrane potential ( $E_m$ ) of H36 cells was measured without inhibitor (Control), and after treating the cells with 5  $\mu$ M E4031 for 3 and 24 h. Transmembrane potential value was also estimated after a 5 min treatment with the inhibitor in extracellular saline containing 140 mM KCl, followed by a 3 h exposition of the cells to E4031 in standard culture medium (3h + KCl pulse).  $E_m$  values of the parental HEK293 and the T2 cells are also shown. Averaged  $E_m$  values for the number of the cells indicated on the bars, were compared with Student  $t$  tests: \* $p < 0.05$ .

**Figure 3.** Cytotoxicity of MMS on different cells. **A** Effect of MMS on cell viability in HEK293, T2 and H36 cells. Data indicate the percentage of cell survival (averaged mean  $\pm$  SEM) measured with the MTS viability assay as indicated in "Material and Methods" section, 24 h after the 3 h treatment with different MMS concentrations. Continuous lines correspond to Hill model fits to the experimental dose-response data, performed with the eeFit add-in for Microsoft Excel [87], as indicated in Methods. **B** Clonogenicity of HEK293 and H36 cells lines upon MMS treatment. Cells were treated as described in Methods. Representative photographs of the plates showing the colonies are presented at the top. Averaged mean  $\pm$  SEM colony formation data from HEK293 (n=6) and H36 (n=9) plates are shown at the bottom, after correcting data with the negative controls, \*  $p < 0.05$  after one-way ANOVA and SNK and/or Tukey post-hoc tests.

**Figure 4.** Comparison of the MMS-induced DNA damage levels in HEK293, H36 and T2 cells, measured with the Comet assay. Left. % Tail DNA averaged values measured after 3 h treatments with the indicated MMS concentrations. Right. Comparison of the DNA damage induced by 0.2 mM MMS (net values of % Tail DNA upon subtraction of the spontaneous DNA damage) in the different cell types (dotted square in the left panel), with one-way ANOVA and SNK post-hoc tests. Mean  $\pm$  SEM values from at least three independent experiments are plotted on the graphs. \*\*  $p < 0.01$ .

**Figure 5.** Comparison of MMS effects on apoptosis levels in HEK293, T2 and H36 cells. **A** Flow cytometry dot plots, for negative control and 0.35 mM MMS concentration treated cells, representative for the different experiments and cell lines. **B** Bar plots showing the MMS-induced early (above) and late (below) apoptosis measured by flow cytometry, 24 h after 3 h treatments with the chemical in each cell line. Mean  $\pm$  SEM values from at least three independent experiments are shown. \*  $p < 0.05$  after comparison with the respective negative controls with one-way ANOVA and SNK and/or Tukey post-hoc tests.

**Figure 6.** MMS effects on cell cycle progression of HEK293, T2 and H36 cells. Plots of cell percentages in G1, S and G2 phases, determined by flow cytometry in every cell type 24 h after a 3 h treatment with the indicated MMS concentrations, are shown at the top. Comparisons of percentage of cells in S (left) and G2 (right) phases in the three cell lines, at each MMS concentration are depicted at the bottom. Mean  $\pm$  SEM values from at least three independent experiments are shown. \*  $p < 0.05$ ; \*\*\*  $p < 0.001$  after comparison with the respective negative controls using one-way ANOVA and SNK and/or Tukey post-hoc tests.

**Figure 7.** Determination of E4031 ability to inhibit Kv11.1 currents in H36 cells. **A** Representative currents during the first depolarization step sequence (top) after membrane patch perforation. Current recordings correspond to untreated cells (negative control), cells incubated 3 or 24 h with 5  $\mu$ M E4031, and cells treated for 3 h with the inhibitor preceded by 5 min with 5  $\mu$ M E4031 in an extracellular saline containing 140 mM KCl. **B** Time course of E4031-induced inhibition of tail currents during the repolarization to -50 mV in response to voltage pulse steps as indicated in panel A, at 20 s intervals. Start of continuous perfusion of the recording chamber with extracellular saline containing 1  $\mu$ M E4031 is indicated by an arrow. Filled circles represent the results from cells incubated 24 h in the presence of 5  $\mu$ M E4031 before beginning the electrophysiological recording in saline with 1  $\mu$ M of the inhibitor. Peak tail current magnitudes are always represented normalized to that obtained in the absence of the inhibitor, according to averaged values presented in panel C. **C** Current densities normalized to cell capacitance in the whole cell population tested. Statistical analysis of E4031 effects were performed with one-way ANOVA and SNK post-hoc tests. \*  $p < 0.05$ .

**Figure 8.** Incubation with E4031 abolished the effects of Kv11.1 expression on MMS-induced cell viability and DNA damage. **A** Effect of E4031 on viability changes induced by MMS in H36 cells. Percentages of cell survival were determined adding 5  $\mu$ M E4031 to the indicated MMS concentrations as described in Methods, and are represented together with those of H36 and T2 cells without inhibitor (from Figure 3). **B** Effect of Kv11.1 current inhibition on MMS-induced DNA damage. % Tail DNA mean values from at least three independent experiments are represented, from H36 and T2 cells treated for 3 h with E4031 and MMS, and preceded by a 5 min period with E4031 in high KCl extracellular saline (KCl), together with data from H36 and T2 cells without inhibitor (from Figure 6). Inset, comparison of DNA damage induced by 0.2 mM MMS (dotted square in the main panel) in the indicated cell types. Data from H36 incubated with E4031 without high-K pre-treatment (H36/E4031), and from T2 and H36 cells pre-treated with the inhibitor in high KCl extracellular saline (E/KCl) were included in the analysis. The respective induced DNA damage from the different cells were compared with one-way ANOVA ( $p = 0.001$ ), and the SNK and/or HSD Tukey post-hoc tests provided the three homology groups represented by horizontal lines.

**Figure 9.** Estimation of DNA repair activity in control HEK293 and Kv11.1-expressing H36 cells. **A** Analysis of DNA damage removal using the Comet assay. Cells were treated with MMS for 3 h and the level of DNA damage was measured after the indicated recovery times. The remaining DNA damage was compared with one-way ANOVA, and the SNK and/or HSD

Tukey post-hoc tests, to provide the two homology groups represented by horizontal lines. **B** Expression of the *PARP1* gene. Expression levels were compared by qPCR as indicated in Methods, to determine fold changes when different cell types and treatment conditions were compared to untreated HEK293 cells. 0.2 mM MMS was used for treatments. \*  $p < 0.05$  versus untreated control HEK293 cells, after one-way ANOVA and SNK and/or HSD Tukey post-hoc tests.

**Figure 1**

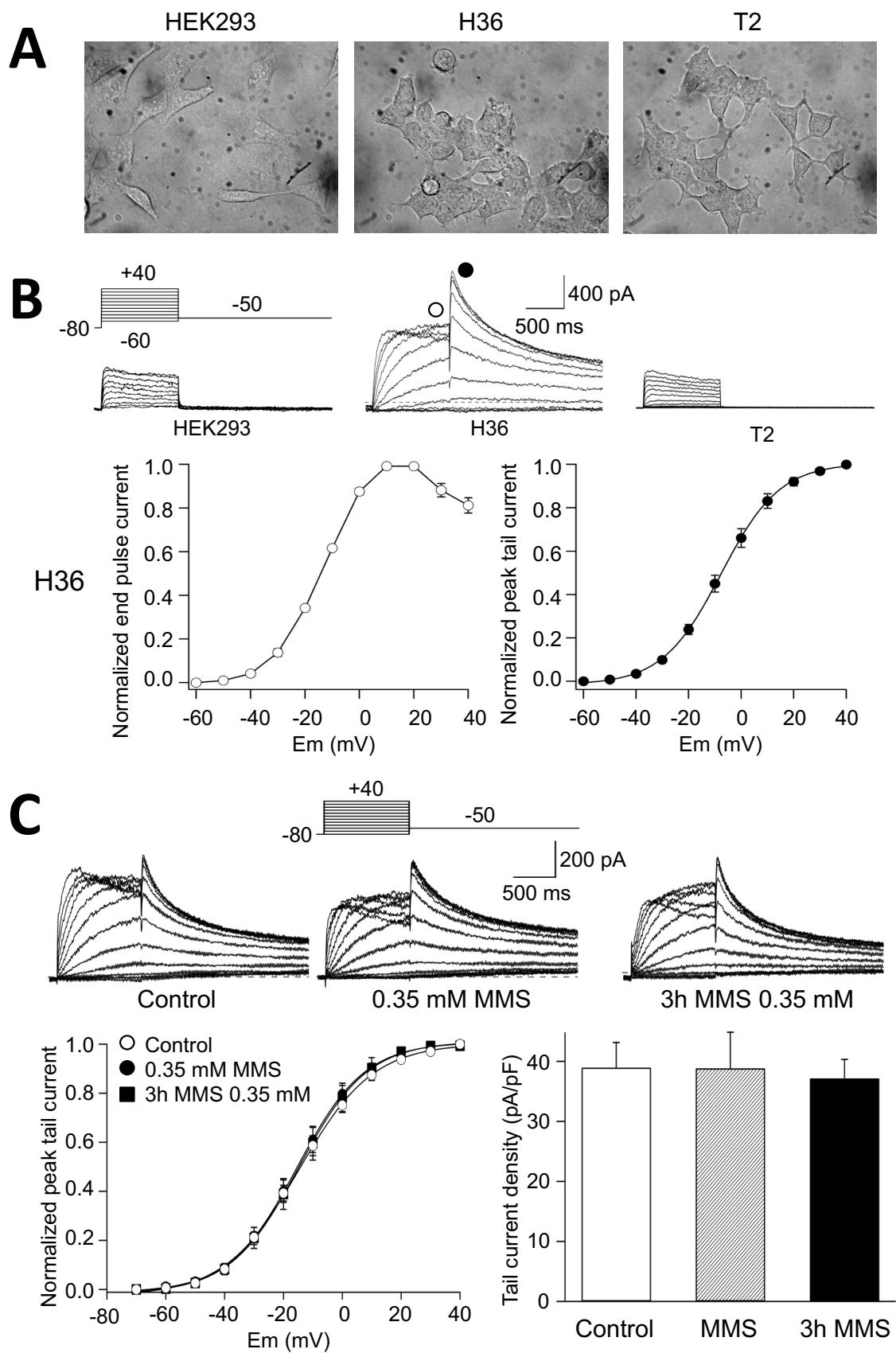


**Figure 2**

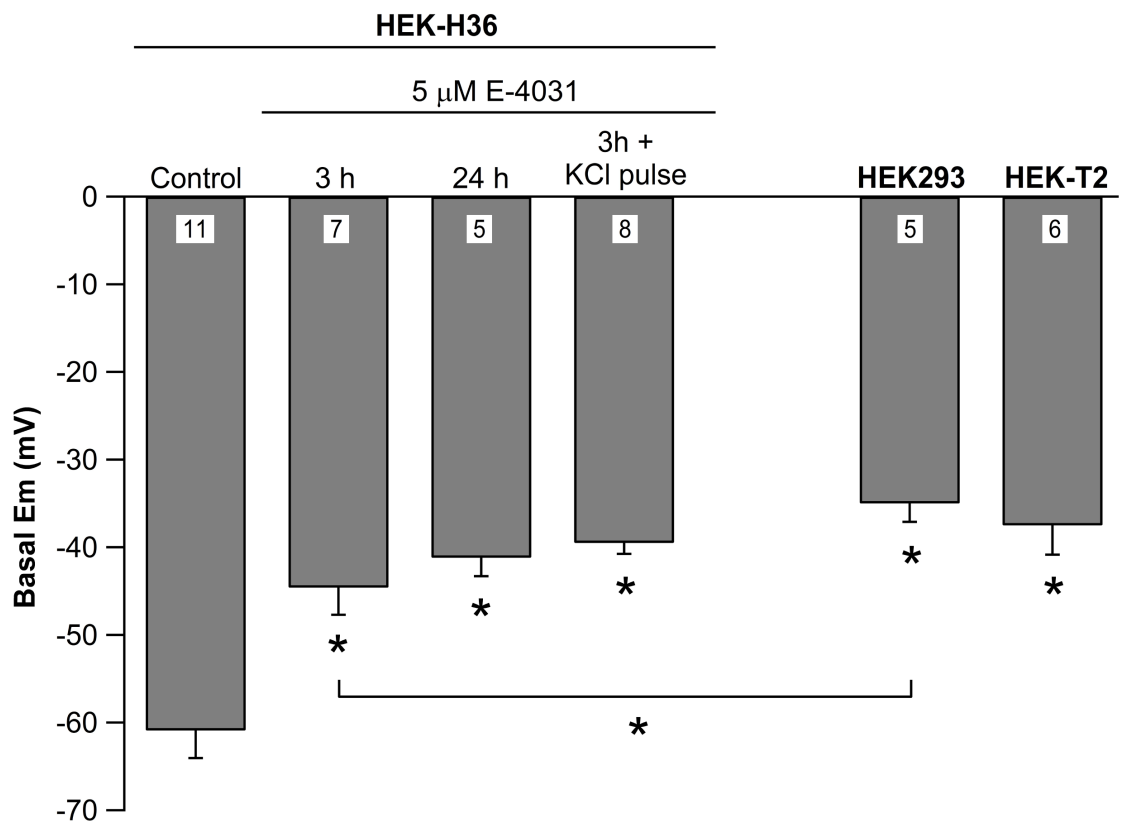
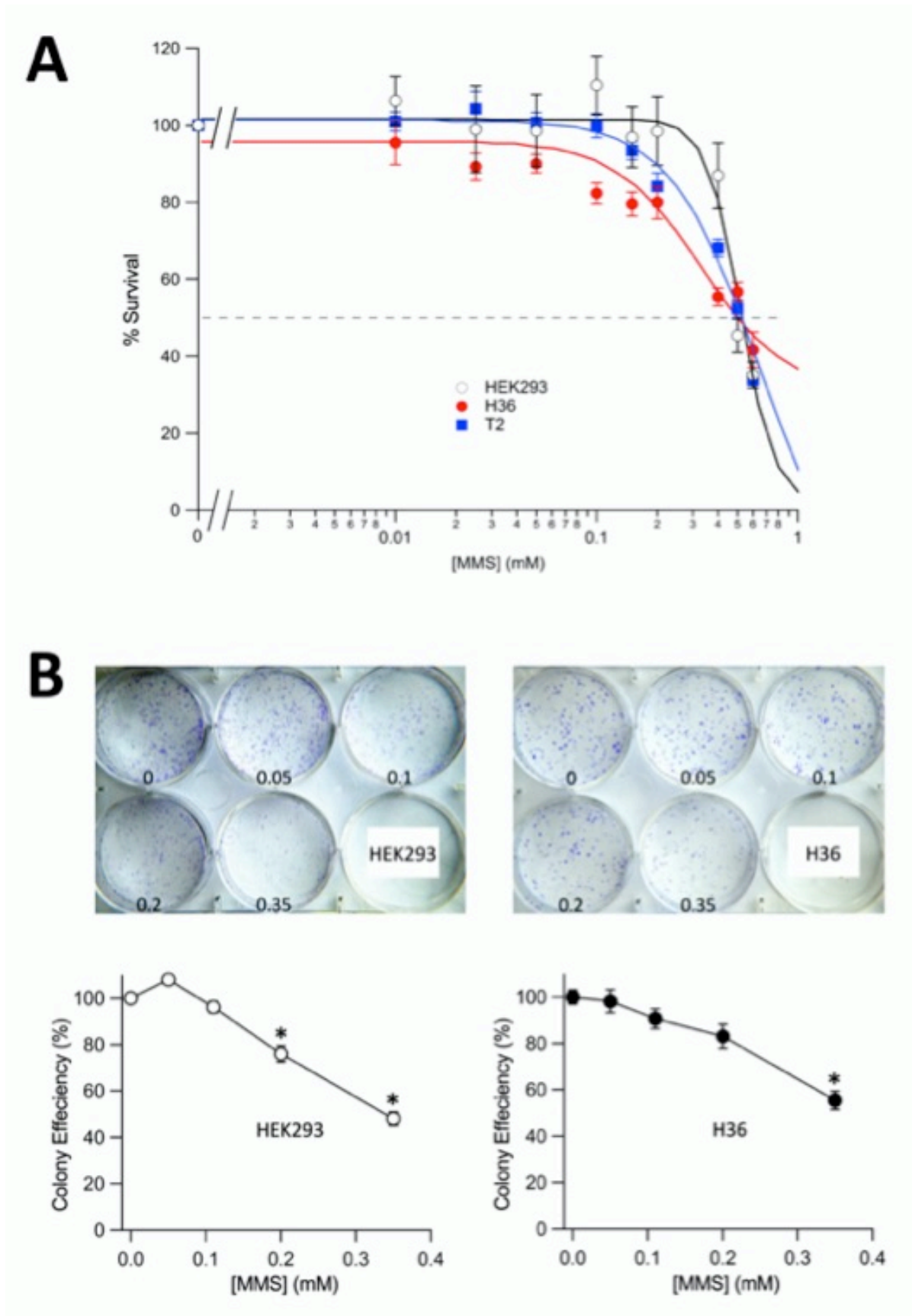
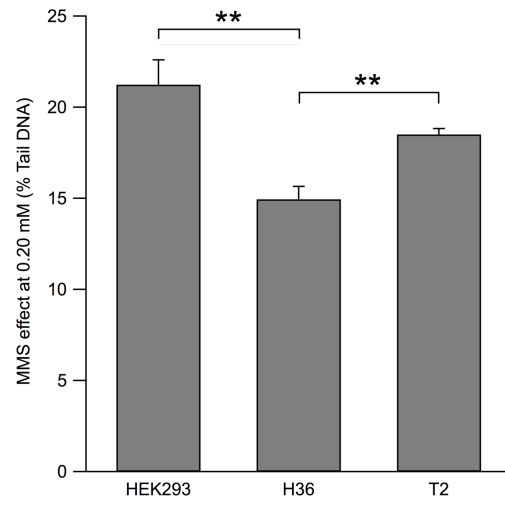
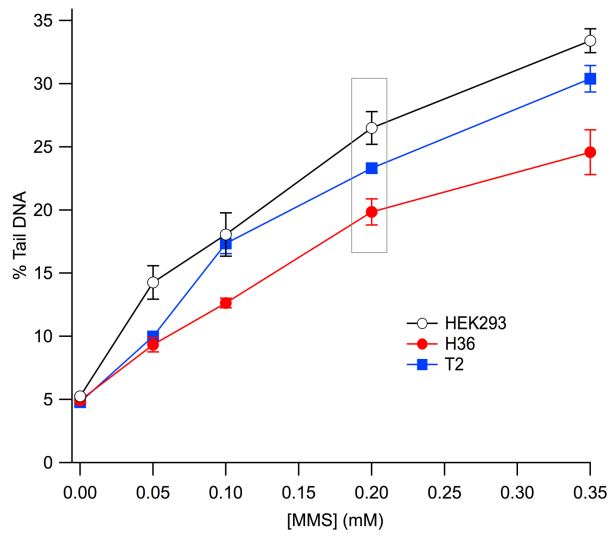


Figure 3



**Figure 4**



**Figure 5**

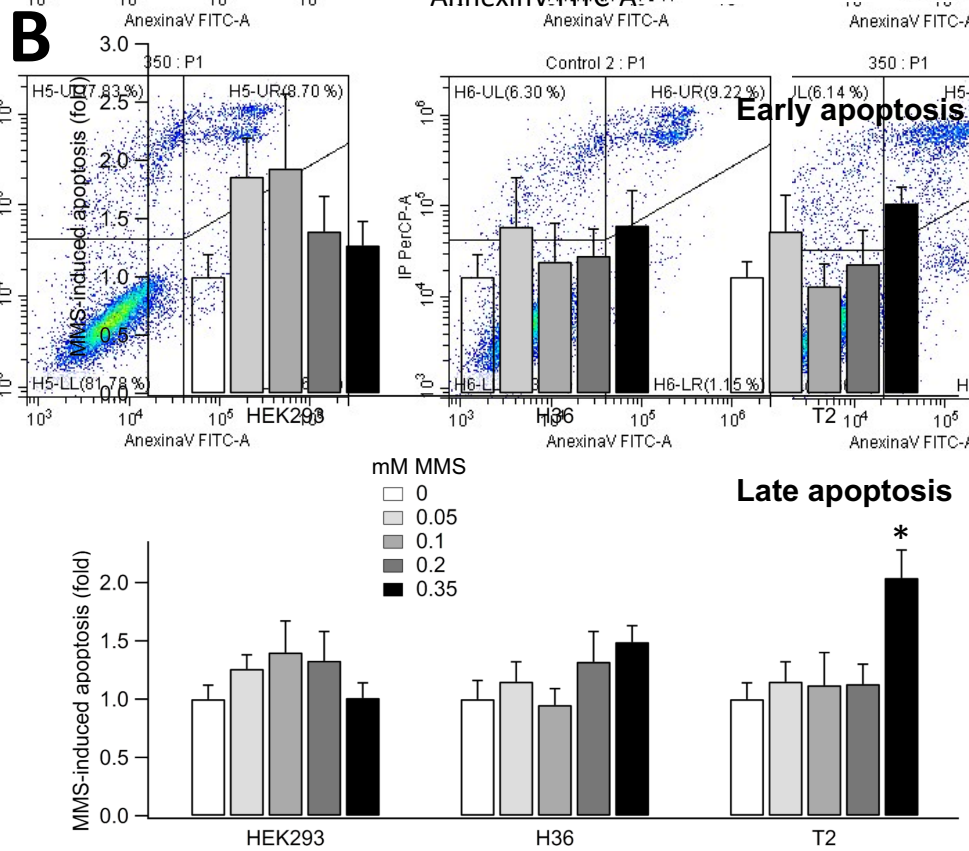
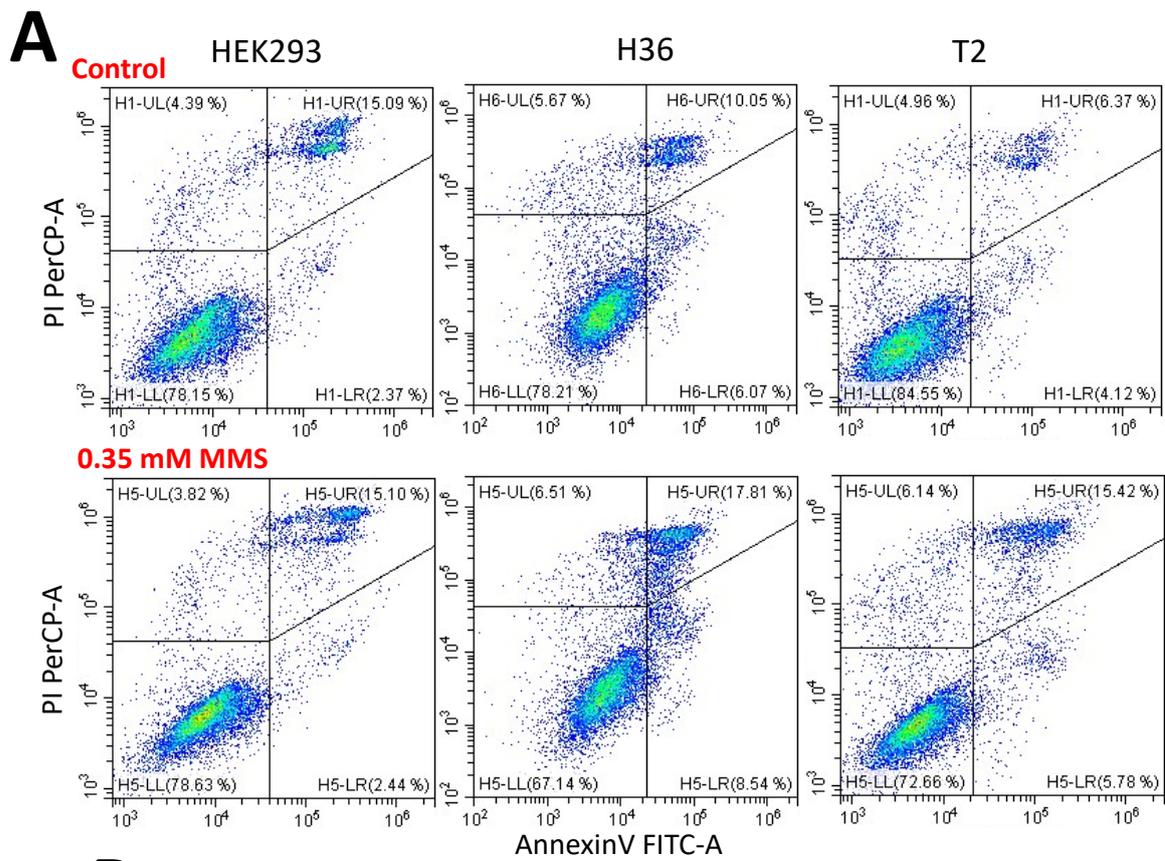


**Figure 6**

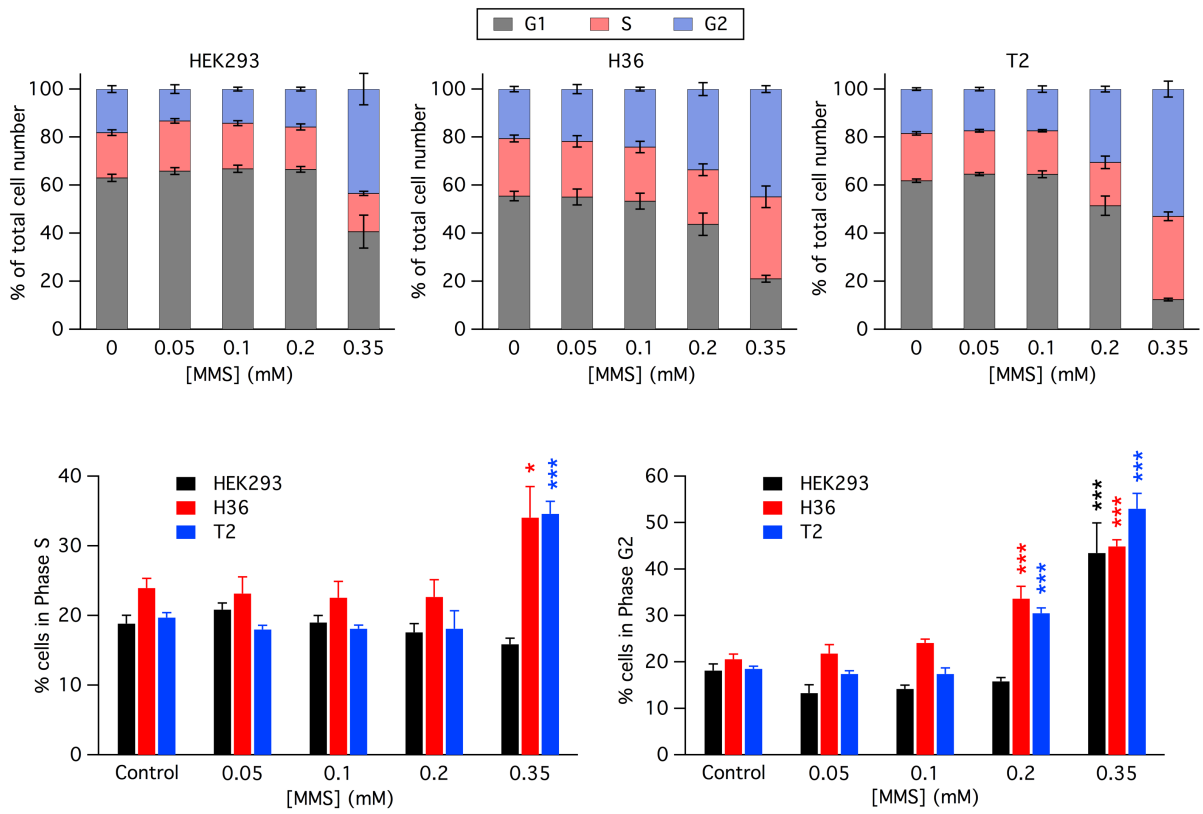


**Figure 7**

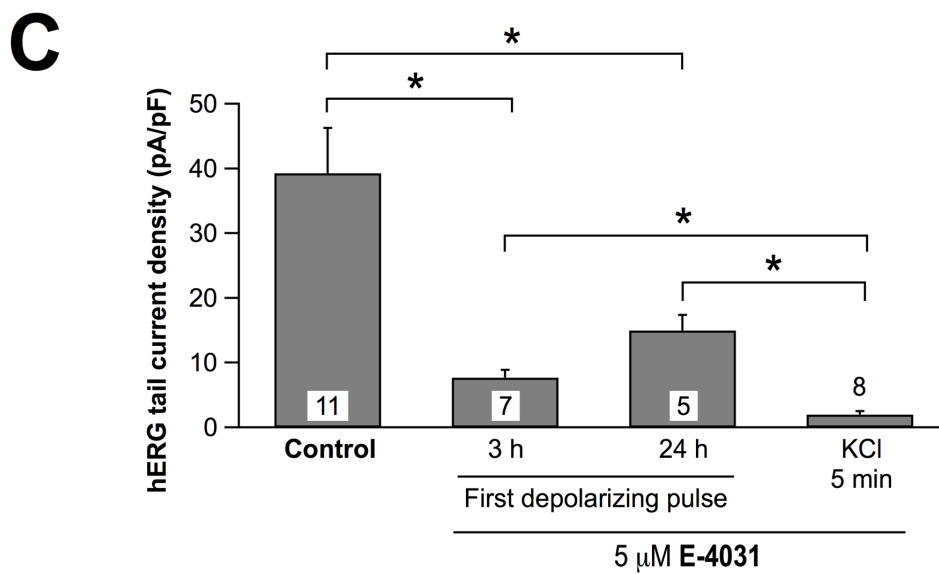
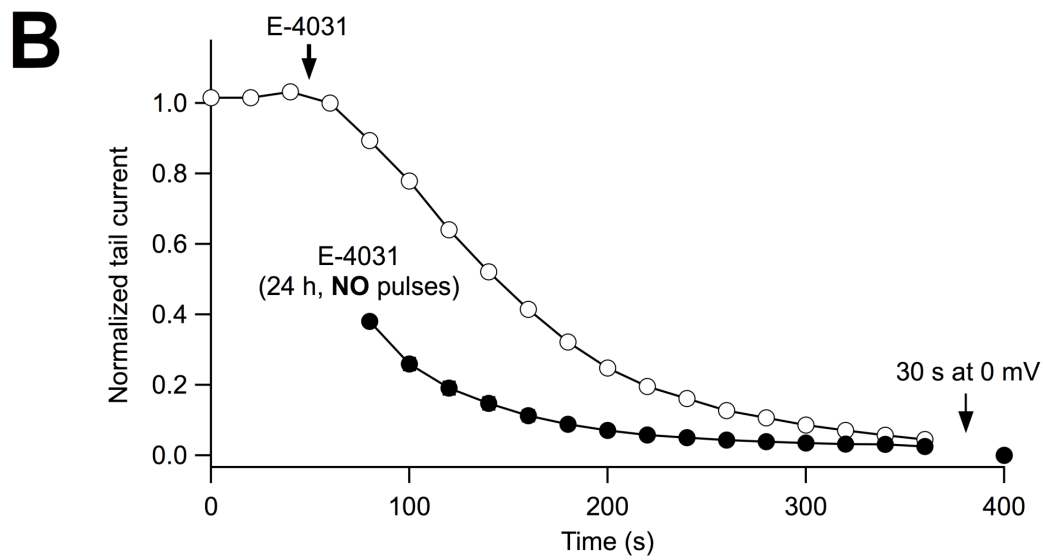
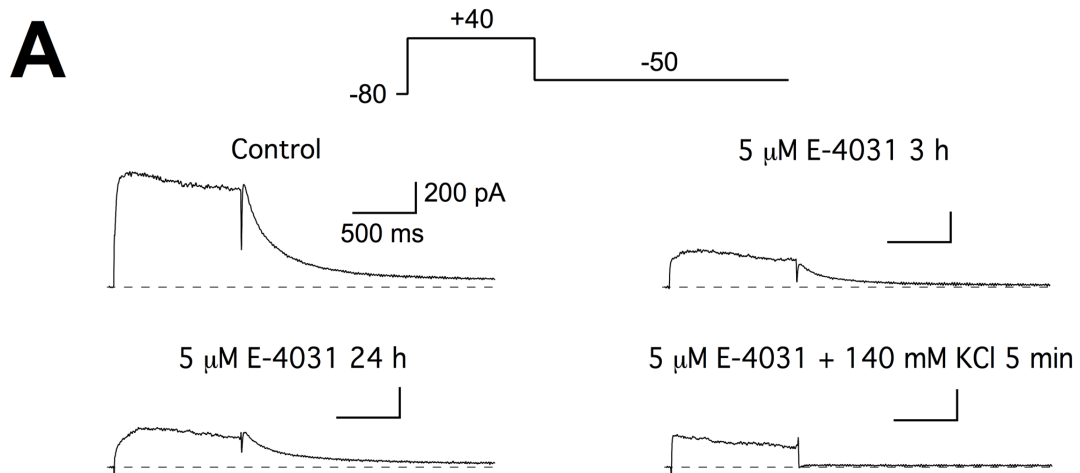


**Figure 8**

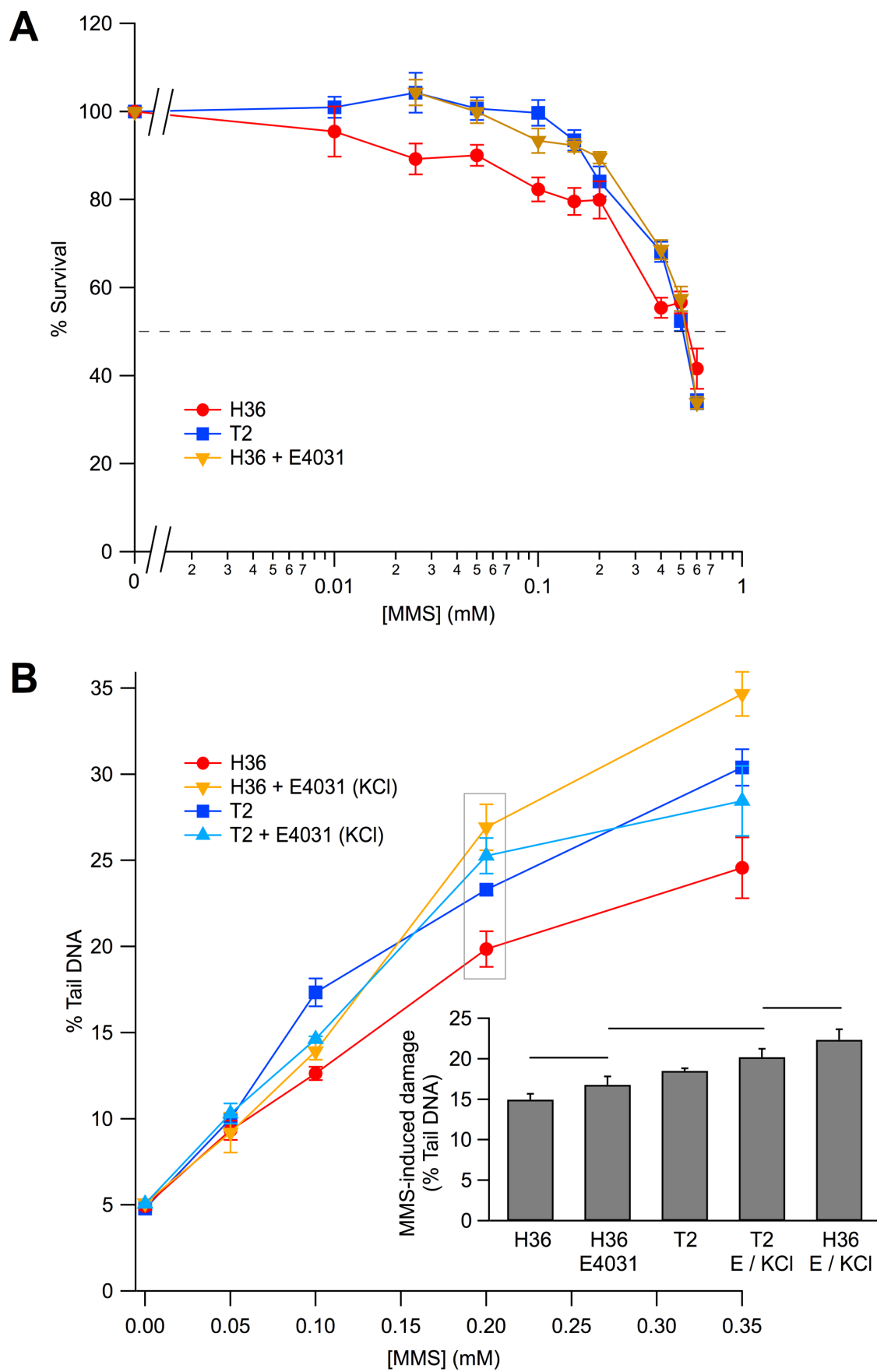
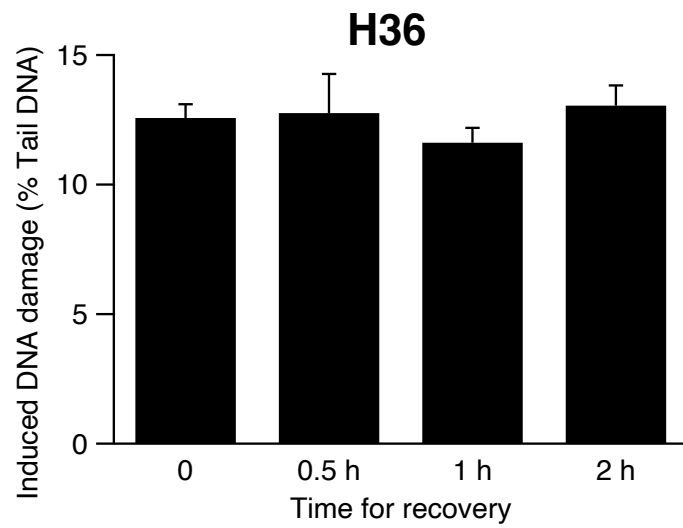
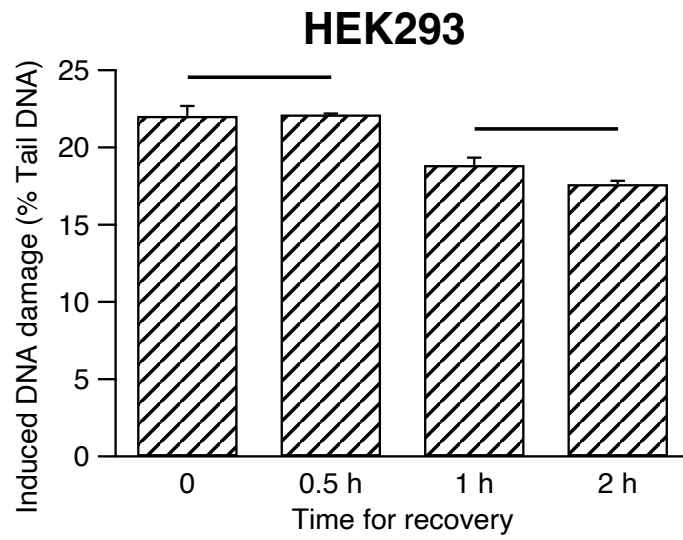


Figure 9

**A**



**B**

